University of Alberta

SINGLE RESISTOR METHODS OF REDUCING INDUCTION GENERATOR INRUSH CURRENT

by

Arash Sharghi

A thesis submitted to the Faculty of Graduate Studies and Research in partial fulfillment of the requirements for the degree of Master of Science.

Department of Electrical and Computer Engineering

Edmonton, Alberta

Fall 2005

Library and Archives Canada

Published Heritage Branch

395 Wellington Street
Ottawa ON K1A 0N4
Canada

Bibliothèque et Archives Canada

Direction du Patrimoine de l'édition

395, rue Wellington
Ottawa ON K1A 0N4
Canada

Your file Votre référence
ISBN: 0-494-09284-X
Our file Notre référence
ISBN: 0-494-09284-X

NOTICE:
The author has granted a non-exclusive license allowing Library and Archives Canada to reproduce, publish, archive, preserve, conserve, communicate to the public by telecommunication or on the Internet, loan, distribute and sell theses worldwide, for commercial or non-commercial purposes, in microform, paper, electronic and/or any other formats.

The author retains copyright ownership and moral rights in this thesis. Neither the thesis nor substantial extracts from it may be printed or otherwise reproduced without the author's permission.

AVIS:
L'auteur a accordé une licence non exclusive permettant à la Bibliothèque et Archives Canada de reproduire, publier, archiver, sauvegarder, conserver, transmettre au public par télécommunication ou par l'Internet, prêter, distribuer et vendre des thèses partout dans le monde, à des fins commerciales ou autres, sur support microforme, papier, électronique et/ou autres formats.

L'auteur conserve la propriété du droit d'auteur et des droits moraux qui protège cette thèse. Ni la thèse ni des extraits substantiels de celle-ci ne doivent être imprimés ou autrement reproduits sans son autorisation.

In compliance with the Canadian Privacy Act some supporting forms may have been removed from this thesis.

While these forms may be included in the document page count, their removal does not represent any loss of content from the thesis.

Conformément à la loi canadienne sur la protection de la vie privée, quelques formulaires secondaires ont été enlevés de cette thèse.

Bien que ces formulaires aient inclus dans la pagination, il n'y aura aucun contenu manquant.

Canada

For Bonnie

Abstract

The induction generator, as an economical form of distributed generator, has received increased attention in recent years. This is because induction generators have advantages over synchronous generators such as lower unit cost, smaller size, less maintenance and better transient characteristics. When induction generators are connected to the grid, large currents are momentarily drawn causing voltage sags. This voltage sag disturbance can lead to equipment failure and is a power quality concern to the users connected to the grid.

The objective of this research was to investigate two new methods of reducing inrush current during induction generator connection to the grid. Experiments and computer simulations were conducted to assess the effectiveness of the two proposed methods. The results show that the proposed methods were effective in reducing inrush current. Effectiveness of the two new methods was measured by comparing the inrush currents with each other as well as with conventional methods.

Acknowledgements

First of all, I would like to thank my supervisor Dr. Wilsun Xu, for providing me the opportunity to write this thesis and for guiding me in my research endeavors. Dr. Xu has been a mentor and teacher to me and I could not have asked for a better supervisor. I would also like to thank the Power Lab technician, Albert Terheide, for his friendship and help. Albert has selflessly shared his knowledge, given technical support and provided me with valuable help and suggestions. Furthermore, I would like to thank Sami Abdulsalam for his help, especially for his suggestions on processing acquired data. I am lucky to have been surrounded by so many friends both in the Power Lab and outside of the lab. These people have made the last two years enjoyable and unforgettable.

In every aspect of my life, my parents have always encouraged and guided me. They have taught me so much and I want to thank them from the bottom of my heart, for all their love and support. I will always be indebted to them.

Last but not least I would like to acknowledge the help and encouragement of my best friend Bonnie Choy. She spent many days and nights helping me edit and revise my thesis. For her friendship and her help, I am truly grateful.

Table of Contents

Chapter 1 Introduction 1

1.1 The Voltage Sag Problem 2

1.2 Induction Generator Background 5

1.3 Solutions to the Induction Generator Connection Problem 7

1.4 Proposed Solutions 10

1.5 Outline of the Thesis 11

Chapter 2 Inrush Current Measurement 14

2.1 Experimental Setup 14

2.2 Direct Connection 19

2.3 Three Series Resistor Method 23

2.4 Summary 25

Chapter 3 Experimental Study of the Proposed Methods 27

3.1 Introduction 27

3.2 Single Series Resistor Method 28

3.2.1 Delta Configuration 28

3.2.2 Delta Configuration Summary 34

3.2.3 Wye Configuration 37

3.2.4 Wye Grounded Configuration 40

3.3 Neutral Resistor Method 43

3.4 Comparison and Conclusion 46

Chapter 4 Simulation Study of the Proposed Methods 48

4.1 Simulation Setup 48

4.2 Single Series Resistor Method 51

4.2.1 Wye Configuration 51

4.2.2 Wye Grounded Configuration 53

4.3 Neutral Resistor Method 54

4.4 Comparison and Conclusion 56

Chapter 5 Steady State Analysis **60**

5.1 Transient Analysis Using Superposition 61

5.2 Unbalanced Induction Machines 66

5.3 Wye Grounded Neutral Steady State Analysis 69

5.3.1 Steady State Equations After Step One 71

5.4 Validation of Steady State Equations 72

5.5 Steady State Voltage and Inrush Current as Rotor Speed Changes 75

5.6 Summary 77

Chapter 6 Conclusions and Future Work **78**

Bibliography **80**

Appendix **84**

List of Tables

Table 2.1: Summary of Direct Connection 22
Table 2.2: Three Series Resistor Summary 25
Table 3.1: Delta Configuration Possible Sequences 29
Table 3.2: Wye Configuration Possible Sequences 38
Table 3.3: Wye Grounded Configuration Possible Sequences 41
Table 3.4: Neutral Resistor Method Possible Sequences 43
Table 3.5: Optimal Sequence and Resistance for Each Configuration at 1800rpm 46
Table 4.1: PSCAD Simulation Parameters 49
Table 4.2: Optimal Sequence and Resistance for Each Configuration at 1800rpm 58
Table 5.1: Relationship Between Steady State Voltage and Inrush Current 65
Table 5.2: Possible Sequences 69
Table 5.3: Simulated Induction Machine Parameters 72
Table 5.4: Experimental Induction Machine Parameters 74

List of Figures

Figure 1.1: Voltage Sag Phenomenon Circuit Diagram 3
Figure 1.2: Sample Inrush Current Waveforms 4
Figure 1.3: Sample Voltage Sag Waveforms at Point of Common Coupling 4
Figure 1.4: Single Line Diagram of Thyristor Soft Starter Method 8
Figure 1.5: Single Line Diagram of Three Series Resistor Method 8
Figure 1.6: Doubly Fed Induction Generator 9
Figure 1.7: Single Series Resistor Method 10
Figure 1.8: Neutral Resistor Method 11
Figure 2.1: Experimental Setup 15
Figure 2.2: Three Possible Stator Configurations 15
Figure 2.3: Sample Transients 17
Figure 2.4: Sample Collection of Data 18
Figure 2.5: Direct Connection Method 19
Figure 2.6: Typical Current Waveforms in one of the Phases 20
Figure 2.7: Direct Connection with Delta Connected Stator 21
Figure 2.8: Direct Connection with Wye Connected Stator 21
Figure 2.9: Direct Connection with Wye Grounded Connected Stator 21
Figure 2.10: Three Series Resistor Method 23
Figure 2.11: Inrush Current Curves for Delta Connected Stator 24
Figure 2.12: Inrush Current Curves for Wye Connected Stator 24
Figure 3.1: Delta Configuration 29
Figure 3.2: Max. Peak Inrush Current in Step One 30
Figure 3.3: Inrush Current at Different Rotor Speeds in Step One, R=4.76Ω 30
Figure 3.4: Max. Peak Inrush Current in Step two 32
Figure 3.5: Maximum Peak Inrush Current in Step Three 33
Figure 3.6: Series Resistor Inrush Current Curves 1800rpm (Delta Configuration) 35
Figure 3.7: Optimization Summary 36
Figure 3.8: Optimal Resistance Value 36
Figure 3.9: Wye Configuration 38
Figure 3.10: Series Resistor Inrush Current Curves at 1800rpm (Wye Configuration) 39

Figure 3.11: Wye Grounded Configuration 41
Figure 3.12: Step One and Two Peak Inrush Current Curves 41
Figure 3.13: Sequence CRBA and CRAB Inrush Current Curves (Wye Grounded Config.) 42
Figure 3.14: Neutral Resistor Method 43
Figure 3.15: Summary of Step One and Two Inrush Current (Neutral Resistor Method) 44
Figure 3.16: Sequence ACBR and ACRB Inrush Current Curves (Neutral Resistor Method) 45
Figure 3.17: Summary of Inrush Current at a Rotor Speed of 1800rpm 47
Figure 4.1: Screen Shots of Simulation Setup in PSCAD 50
Figure 4.2: Simulated Inrush Current Curves (Wye Configuration) 52
Figure 4.3: Step One and Two Inrush Current Curves (Wye Grounded Configuration) 53
Figure 4.4: Sequence CABR and CARB Inrush Current Curves (Wye Grounded Config.) 54
Figure 4.5: Step One and Two Inrush Current Curves (Neutral Resistor Method) 55
Figure 4.6: Sequence ABCR and ABRC Inrush Current Curves (Neutral Resistor Method) 56
Figure 4.7: Summary of Inrush Current at a Rotor Speed of 1800rpm 57
Figure 4.8: Optimal Resistance versus Rotor Speed 58
Figure 4.9: Maximum Peak Inrush Current versus Rotor Speed 59
Figure 5.1: Wye Grounded Configuration with Series Resistor After Step One 61
Figure 5.2: Simplified Circuit with only Phase C Closed 62
Figure 5.3: Application of Superposition when Closing Contactor A in Step Two 63
Figure 5.4: Equivalent Circuit when Closing Contactor A in Step Two 63
Figure 5.5: Steady State Voltages and Inrush Current Associated with Step Two 64
Figure 5.6: Induction Machine Symmetrical Component Equivalent Circuits 67
Figure 5.7: Single Series Resistor Method with Grounded Neutral Configuration 69
Figure 5.8: Steady State Voltage and Current after Step One 73
Figure 5.9: Delta V_a as a Function of Rotor Speed, Series Resistor R=0.1785 Ω 76
Figure 5.10: Steady State Voltage prior to Closing A and Max. Peak Inrush after Closing A 76
Figure A1: Steady State Voltage and Current After Step two 86
Figure A2: Steady State Voltage and Current After Step Three 87

List of Symbols

a	$e^{j\frac{2\pi}{3}}$
DFIG	doubly fed induction generator
DC	direct current
$e_{a,b,c}$	stator terminal-ground voltage (rms)
$E_{a,b,c}$	source phase-ground voltage (rms)
FLA	full load amps
HP	horse power, 746 Watts
$i(t)$, I	current
L	inductance
λ	point in supply cycle on connection
MPIC	Maximum Peak Inrush Current
MTTF	mean time to failure
PCC	point of common coupling
pu	per unit
PF	power factor
R	resistance
R_1	stator resistance
R_t	system resistance
R_2	rotor resistance
rpm	revolutions per minute
rms	root-mean-square
s	slip
t	time
V	voltage (rms)
VA	volt-amps
ω	system angular frequency ($2\pi f$) (rad/sec)
ω_r	rotor angular frequency (rad/sec)
WRIM	wound rotor induction machine
X	reactance

X_l	stator leakage reactance
X_t	system reactance
X_m	generator magnetizing reactance
X_2	rotor leakage reactance
Z	Impedance, R+jX

Chapter 1

Introduction

In the past, society has relied heavily on traditional methods of power generation, where large power plants mainly use fossil fuels to generate power for consumers. In 1999, 62% of the world's power was generated from non-renewable resources such as natural gas, oil, and coal [1]. These are finite commodities with byproducts that may be harmful to the environment. Deregulation of the electricity market has provided the industry with opportunities to develop smaller scale generation units that tend to derive its energy from more environmentally friendly, readily available sources such as wind power, hydro power and solar power. With these resources so widely dispersed throughout the land, it is favorable to have smaller, more dispersed generation units to harness these resources. The use of multiple generator units also allows for greater reliability, because one small unit failing has less severe consequences than if one large unit were to fail. Dispersing smaller generation units across the power grid and closer to consumers is referred to as distributed generation. Distributed power generation can provide cost effective, reliable power in an environmentally friendly manner. As a result, the use of distributed power generating units has significantly increased in the past few years [2].

A type of generator that is commonly used as a distributed generator is the induction generator. Induction generators have inherent advantages over synchronous generators such as low unit cost, smaller size, less maintenance and better fault transient characteristics [3, 4, 5]. As a result, induction generators have received more attention than other types of generators and have been widely employed in grid-connected hydroelectric and wind energy applications [3].

When an induction generator is first connected to the grid, large currents are momentarily drawn. This transient current is often referred to as inrush current. Inrush currents can cause the voltage at a given point to momentarily drop below normal root-mean-square (rms) values. This phenomenon is commonly known as "voltage sag" or a "voltage dip". Voltage sag disturbances in industrial settings can cause equipment to fail and has negative consequences, such as lost opportunity and poor quality in the finished product.

Voltage sags can be detrimental to industrial processes. In fact, voltage sags are the most important power quality problem facing many industrial customers [6]. Some examples of industrial equipment that are sensitive to voltage sags are: Motor Contactors, High-Intensity Discharge (HID) lamps, Adjustable Speed Motor Drives (ASD) and Programmable Logic Controllers (PLC's). PLC's often automate industrial processes and are one of the most important parts of an industrial process negatively affected by voltage sags. Malfunctions in PLC's may cause an entire process to shut down. Once the PLC supply voltage has dropped to a certain value for a given duration, the equipment will fail. Different categories of equipment will have different sensitivities to voltage sags [6]. For example, some PLC equipment will fail when there is a voltage drop as low as 10% that lasts for only a few cycles [7]. Furthermore, a significant voltage drop could cause induction motors connected to the system to lose rotational speed and draw more current to compensate [8]. This increase in drawn current will further intensify the voltage sag in the system that was initially caused by the induction generator inrush current.

Voltage sags due to induction generator connection is a serious problem. Fortunately, by reducing the inrush current, the voltage sag can also be reduced. This chapter will explain why inrush current causes voltage sags and the problems associated with voltage sags. Some common methods to reduce inrush current when connecting induction generators are introduced in section 1.3. Section 1.4 presents two novel, cost effective methods that can be used to prevent voltage sags.

1.1 The Voltage Sag Problem

One of the problems with connecting induction generators to a power system is that it draws high inrush current. Induction generators draw large transient inrush currents several times as large as the machine rated current at the instant they are connected to the grid [9,10]. These high inrush

currents, if large enough, can cause voltage sags to occur [11]. A voltage sag has been defined as a reduction in rms voltage, with a duration between 0.5 cycles and 1 minute [12]. Voltage sags are dependent on the proximity to the site where large currents are drawn [13] as well as the magnitude of the current. Although voltage sags are usually caused by a remote fault somewhere in the power system [6], they are also caused by the energization of large loads, such as induction generators.

In North America, power is transmitted through three phase transmission lines. As a result, most generators connected to the grid are three phase generators. Under normal conditions, all three phases of a transmission line and generator are generally the same. Therefore, it is common to describe the power system using only one of the phases in a single line diagram. A single line diagram demonstrating the voltage sag phenomenon is shown in Figure 1.1. At the instant the generator is connected to the grid, inrush current is drawn by the induction generator in all three phases. This naturally causes a voltage to be dropped across the line impedances R and jX_L in each phase. If the inrush current is large enough, the customer will experience a momentary drop in voltage, and any equipment connected to the point of common coupling will be affected. The PCC is the point in the power system where customers are connected.

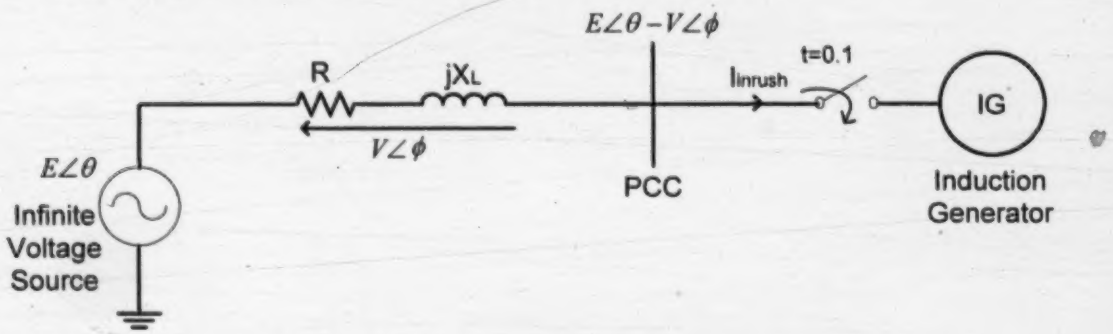

Figure 1.1: Voltage Sag Phenomenon Circuit Diagram

Figure 1.2 illustrates the induction generator inrush current when an induction generator is connected to the grid at synchronous speed. Figure 1.3 shows the voltage at the PCC prior to and after the breaker is closed. The breaker is closed at 0.1 sec.

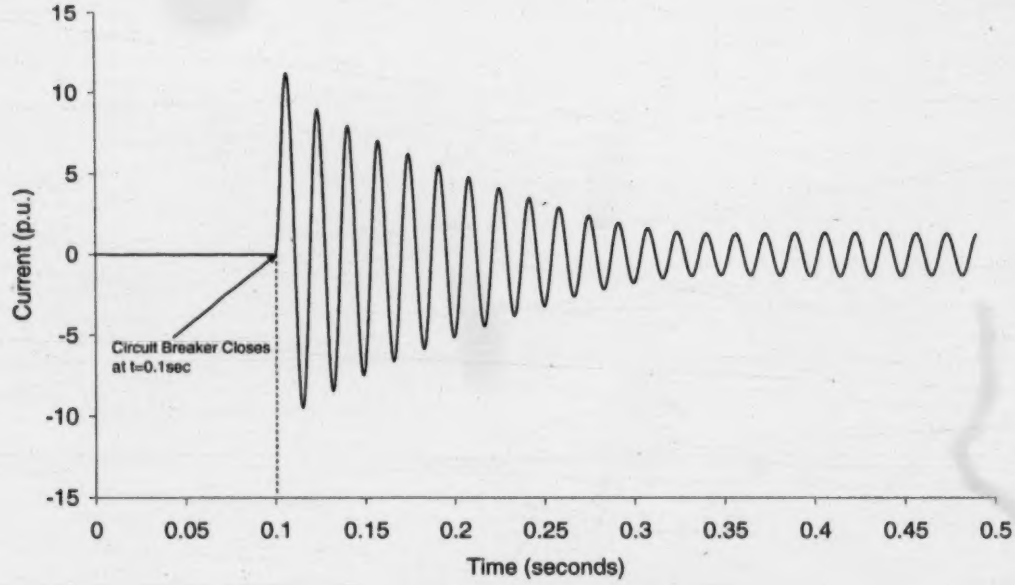

Figure 1.2: Sample Inrush Current Waveforms

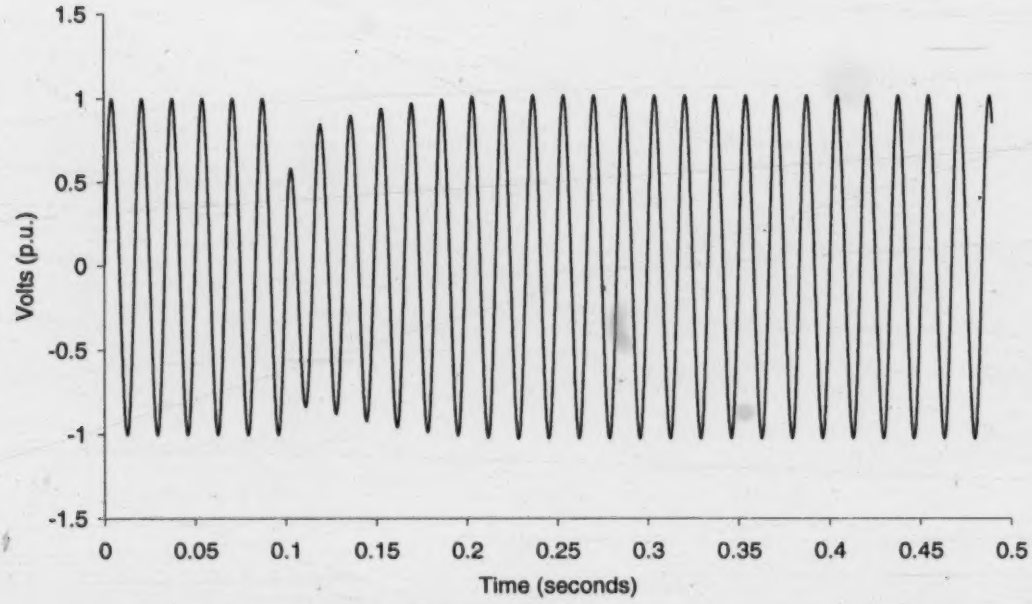

Figure 1.3: Sample Voltage Sag Waveforms at Point of Common Coupling

The current and voltage in the previous two figures has been presented in per-unit (pu). Under normal conditions, the peak voltage is 1pu. When the induction generator current is large, the

peak voltage at the PCC drops below 1pu, affecting any customers connected. Once the induction generator current dies down and reaches steady state, the voltage at the terminal returns back to 1pu. The larger the peak inrush current, the larger the voltage sag. It should be noted that the previous figure shows inrush current and corresponding voltage sag of only one of the phases. Similar results would be found for all three phases of the system.

1.2 Induction Generator Background

The three phase induction machine, sometimes referred to as an asynchronous machine, was invented by Nikola Tesla in the late 1800's. Since then, it has become the most widely used industrial machine. This is due to its advantages over other electric machinery including DC machines and synchronous machines. Induction machines are cheaper to construct, easier to maintain, and only require a three phase voltage source for them to operate.

Induction machines can be operated as a generator or a motor. An induction generator converts mechanical energy into electrical energy and an induction motor converts electrical energy into mechanical energy. In the past, induction machines have been primarily used as motors. However, distributed generation has gained popularity and so has the demand for cheap and simple methods of generation. As a result more and more induction machines are being utilized for generating purposes. The speed of the rotor defines whether the induction machine is in generating or motoring mode. If the rotor speed is less than synchronous speed, it operates as a motor and if the rotor speed is more than the synchronous speed, it operates as a generator [4,14]. The synchronous speed of a motor is defined by the electrical frequency of the stator voltage and currents, and the number of poles (P) in the machine. It is given in revolutions per minute (rpm) in the following formula:

$$\text{Synchronous speed (rpm)} = \frac{120 \cdot f}{P} \qquad (1.1)$$

The basic theory of induction generators is given in many textbooks and papers. The induction machine consists of two major components: stator and the rotor. The stator, as the name implies, is stationary. It is composed of copper windings arranged specifically in a ferromagnetic material, such that when a balanced set of three phase voltages are applied to these copper windings, a rotating magnetic field is established. The rotating magnetic field rotates with constant magnitude at synchronous speed. The stator surrounds a cylindrical rotor and they are separated by a small

air gap. The rotating magnetic field of the stator produces magnetic flux in the air gap between the stator and the rotor [15]. This flux induces voltage in the rotor bars which in turn causes current to flow. The current in the rotor bars produce a magnetic field in the same way the stator current induces a magnetic field. The interaction between the stator and rotor magnetic fields produces a mechanical torque that rotates the rotor in the same direction as the rotating magnetic field. Anything connected to the rotor will also rotate as long as the induced motor torque is large enough to rotate the load connected to the rotor. In steady state, the motor will spin at some speed lower than the synchronous speed. The larger the load connected to the rotor, the slower the speed of the rotor. If the rotor is connected to a prime mover such as a hydro turbine or wind turbine, the rotor can be driven faster than the synchronous speed. When this occurs, the relative motion of rotor currents and rotor magnetic field is opposite to that of the motor [15]. As a result the rotational energy of the rotor is transferred to the stator and electrical power flows through the stator windings and into the three phase power system [15]. This is known as generation.

It should be noted that there are two types of three phase induction machines: the squirrel cage induction machine and the wound rotor induction machine (WRIM). The main difference between the two machines is that the WRIM can have external connections to the rotor, allowing external control of the rotor currents. The WRIM is more expensive and requires more maintenance than the squirrel cage machine. The methods to reduce inrush current discussed in this work apply to both types of machines except where specifically mentioned.

The general procedure for connecting induction generators to the grid is to allow the prime mover to first accelerate the rotor to near synchronous speed and then electrically connect the stator to the power grid. The closer the machine is to synchronous speed, the shorter the duration of the inrush current [16], thus a shorter voltage sag duration.

Once the induction generator is connected to the grid, the machine can convert mechanical energy from the prime mover to electrical energy, which is then supplied to the grid. In order for this power conversion to occur, the induction machine requires steady state reactive power to establish the magnetic field across the air-gap of the machine [4,17]. The induction machine cannot produce its own reactive power and as a result, reactive current is drawn from the grid to magnetize the machine. This drawn current lowers the power factor (PF). Low PF is a power quality concern and can be avoided by connecting shunt PF correction capacitors. These PF

correction capacitors are often connected to the terminals of the generator to reduce reactive current drawn from the grid and improve PF. It has also been found that PF correction capacitors can reduce induction generator inrush current [18].

1.3 Solutions to the Induction Generator Connection Problem

Decreasing inrush current of induction generators reduces the magnitude and duration of voltage sags and thereby reduces the chances of equipment failure. There are a number of existing ways to reduce inrush current:

Thyristor Soft Starter

The current in an induction machine is proportional to the applied voltage. If large inrush current occurs, it can be prevented by lowering the voltage. The operating principle of a thyristor soft starter is to provide a gradual increase in the induction generator stator voltage which allows the current to be limited. This is accomplished by using two anti-parallel thyristors in each phase as shown in Figure 1.4. By sending delayed signals to the thyristors, the voltage at the generator can be controlled. Once the machine is at full voltage, the soft starter is no longer necessary and is bypassed to avoid thyristor voltage drops. It has already been mentioned that induction generators often require power factor correction capacitors to improve the power quality of the grid. When using the thyristor soft starter, the PF correction capacitor bank is connected to the terminal *after* the thyristors are bypassed (see Figure 1.4). The reason the capacitor is not connected for the entire process is because capacitors used today cannot handle large harmonics that are created by the soft starter [18]. This type of soft-starter can connect an induction generator at 5-30% below the synchronous speed of the generator [18]. A problem with this method is that the current becomes highly distorted while the thyristors are switching [19] which may lead to poor power quality.

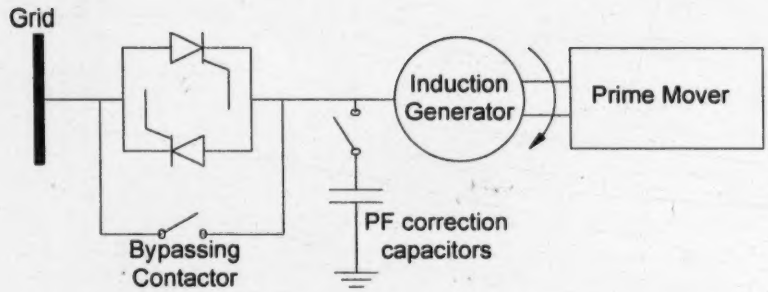

Figure 1.4: Single Line Diagram of Thyristor Soft Starter Method

Three Series Resistor Method

A more cost effective way to reduce inrush current requires the use of 3 resistors in series between the system and induction generator (see Figure 1.5). This increases the load resistance, which decreases the amount of current. Once the induction generator is sufficiently magnetized, the resistors are bypassed. For this method, it is most beneficial to connect close to synchronous speed.

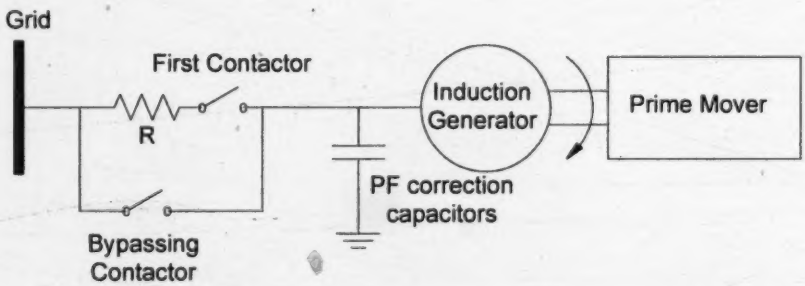

Figure 1.5: Single Line Diagram of Three Series Resistor Method

The main advantage of the external resistor method over the thyristor soft starter method is that PF correction capacitors can be connected to the machine throughout the connection procedure. After the first contactors are closed, the capacitors supply reactive current to the machine. This reduces the amount of reactive current supplied by the grid, thereby reducing the voltage across the resistor. The low voltage across the resistor implies that a small inrush current will be drawn when the resistors are bypassed. Thus, the simple external resistor method gives a lower grid impact than the expensive, power electronic based soft starter [18]. On the other hand, one advantage of the soft starter is that it can connect the generator to the grid much faster than the

resistor method because it can connect at lower speeds. It should be noted that inrush current can be reduced (using the three external resistor method) without the connection of PF correction capacitors. However, it is not as effective (as with the PF correction capacitors installed) since the voltage across each resistor will be larger, leading to a larger inrush current when the resistors are bypassed.

Doubly Fed Induction Generator

A new scheme that is being used for large wind turbine installations is the doubly fed induction generator (DFIG). The DFIG is constructed from a wound rotor induction machine so that the rotor voltage and current can be controlled as shown in Figure 1.6. One advantage of the DFIG over squirrel cage induction machines is that they do not require additional grid connection devices such as a thyristors or resistors [20]. Also, grid synchronization is possible at any operational speed [20].

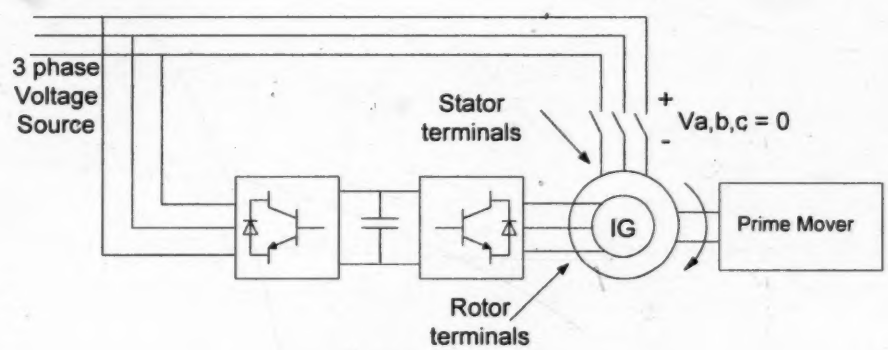

Figure 1.6: Doubly Fed Induction Generator

The connection procedure of a doubly fed induction generator (DFIG) is described in [20]. By controlling the rotor voltages and currents, the voltage induced in the stator windings can be synchronized with the grid. Therefore, the voltage difference across the open contactors can be set to zero at the time of connection. The outcome of the connection process is that it takes about one second and it results in very little inrush current. The DFIG provides a connection to the grid that is softer and faster than the three series resistor method and the thyristor soft starter method. However, the overall cost of the wound rotor induction machine, including the extra equipment such as switching devices, make this scheme expensive.

Other Methods of Minimizing Voltage Sags

Limiting inrush current in an induction generator is not the only approach to preventing voltage sags. By controlling the bus voltage, the result is a stabilization of voltage rather than a mitigation of inrush current. Other ways in which voltage sags can be prevented are listed below.

I. Series Compensation
II. Uninterruptible Power Supply (UPS) [21]
III. Voltage Regulators [6,21]
IV. Inject Series Voltage or Shunt Current [22]

1.4 Proposed Solutions

The purpose of this thesis is to present and investigate two new methods of connecting induction generators to the grid. These new methods minimize inrush current and as a result reduce voltage sags. The proposed methods provide cost effective ways of improving power quality of a power system, using only one resistor and one bypassing contactor rather than three, as with older methods. The two new methods are called the *single series resistor method* and the *neutral resistor method.*

The *single series resistor method* uses only one resistor in series with one of the generator terminals (see Figure 1.7). The *neutral resistor method* requires a resistor at the neutral terminal of a wye connected induction generator (see Figure 1.8). These methods both use sequential closing of the contactors (A,B,C,R) rather than a simultaneous connection of all terminals to the grid.

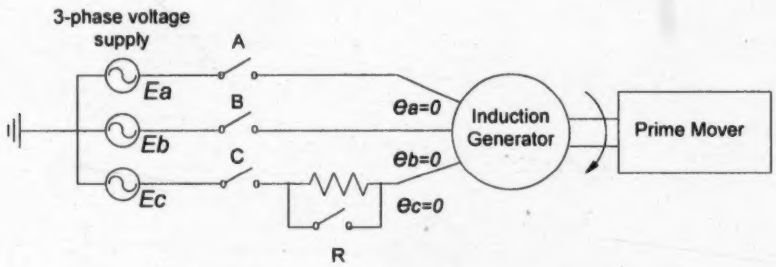

Figure 1.7: Single Series Resistor Method

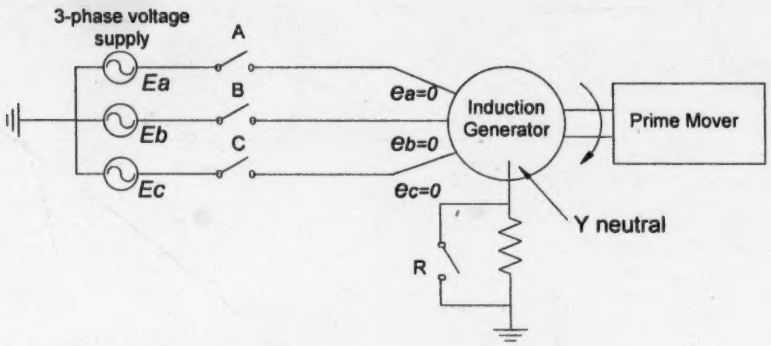

Figure 1.8: Neutral Resistor Method

When all the contactors are open, no current flows in the induction generator stator windings. As a result, there is no voltage induced in the stator windings prior to connection. This is shown in Figure 1.7 and Figure 1.8. The magnitude of the inrush current will be determined by the resistor size and the sequence of switch closure. As each switch is closed, current will flow through the machine. This current will cause a voltage to be induced at the open terminals of the generator. The key to both methods is the sequential closing of the switches, which allows for a gradual magnetization of the generator.

These methods are more cost effective than the traditional 3 series resistor method because they use only 1 resistor and 1 bypassing contactor. This reduces material costs, and will also increase the mean time to failure (MTTF), since there will be fewer components that could possibly malfunction. Cost effective methods to reduce inrush currents and maintain suitable power quality levels will be valuable to power producers and will benefit consumers.

1.5 Outline of the Thesis

Traditional methods of reducing inrush current in induction generators already exist. However, these methods can be expensive and, as a result, are not economical in many situations. For example, smaller companies in deregulated economies may not be inclined to install a wind farm due to high initial cost. It is therefore necessary to minimize the fixed cost of induction generator installations. One way to reduce this fixed cost is to use economical methods of connecting induction generators to the grid. Two new methods of connecting induction generators to the grid have been proposed. The objective of this thesis is to present the usefulness of these two new methods and to analyze why these methods are effective. This is done experimentally by

conducting laboratory tests and theoretically using computer simulation[1]. The following is an outline of the thesis.

There are two purposes of chapter 2. The first goal is to familiarize the reader with the experimental procedure that was used in this thesis. The experimental setup and procedure that was used for all laboratory tests is described. The experimental procedure was used to determine the maximum peak inrush current under different circuit conditions. The second goal is to present results that were obtained when connecting an induction generator to the grid using two traditional methods: *direct connection method* and the *three series resistor method.* Chapter 2 shows that directly connecting the induction generator to the grid causes large inrush current. The peak inrush current using the direct connection method and three series resistor method is found experimentally. Tests were conducted at different rotor speeds to test the correlation between rotor speed and inrush current. It was found that the *three series resistor* method can reduce peak inrush current substantially if the correct resistance values are selected. The optimal resistance value for minimizing peak inrush current was determined experimentally and is reported in this chapter.

Experimental results on the two new proposed methods are presented in chapter 3. The experiments were conducted to determine the maximum peak inrush current. This was achieved using the procedure outlined in chapter 2. Both proposed methods consist of closing contactors sequentially. As a result, multiple sequences are possible when connecting the induction generator to the grid. The sequence that best minimized the inrush current was determined. This sequence is referred to as the "optimal sequence". For the optimal sequence, an "optimal resistor" value was found experimentally. The optimal resistor value is the resistance that best minimizes the maximum peak inrush current. The two proposed methods are compared to the direct connection and three series resistor method.

To complement the experimental results, computer simulation results are provided in chapter 4. The computer simulation was conducted on a 2MVA induction generator. Chapter 4 provides results using the direct connection, three series resistor and the two proposed methods. For the proposed methods, the optimal sequence and corresponding optimal resistor value was found. All four methods are compared.

---

[1] The computer simulation software used in all simulations was PSCAD.

Chapter 5 relates the inrush current in an induction machine with the steady state voltage prior to switch closure. Using superposition, the inrush current (for the single series resistor method with a wye grounded configuration) is described mathematically. This chapter shows that the optimal sequence can be obtained analytically knowing only the steady state voltage across the contactors prior to closing. Steady state equations (for the single series resistor method with a wye grounded configuration) are derived in this chapter. The derivation uses the method of symmetrical components. The equations are verified by comparing the steady state currents and voltages with simulation results.

In chapter 6, the research results are summarized and suggestions for future research are given.

Chapter 2

Inrush Current Measurement

The first section of this chapter will describe the experimental setup that was used for all laboratory experiments in this work. The second and third section will contain experimental results obtained when connecting induction machines to the grid using traditional methods. The traditional methods that are discussed here are the direct and three series resistor connection. Both traditional methods were tested without the installation of PF correction capacitors.

2.1 Experimental Setup

Voltage sags are directly related to the inrush current. The effectiveness of the proposed methods can therefore be evaluated by measuring the inrush current. This is accomplished by capturing inrush current waveforms and extracting the peak inrush current from each waveform. From the extracted results, the maximum peak inrush current can be extrapolated. This section describes the experimental procedure that was designed to determine the inrush current that would cause the worst possible voltage sag.

The experimental equipment used in these experiments consisted of an induction machine, a synchronous machine, and a DC machine. The shaft of each of the 3 machines was coupled together. The synchronous machine and DC machine were used strictly to emulate the performance of a prime mover for the induction generator. The synchronous machine was run at a constant speed of 1800rpm. The DC machine rotor speed could be varied, allowing the

induction machine to be connected to the grid at any rotor speed. All experiments were done with the rotor spinning in the same direction. Current probes, LABView Data Acquisition equipment and Power Quality Troubleshooter Software were used to capture the induction generator inrush current drawn when the induction generator was connected under varying conditions. These variations include the rotor speed and resistance value. The sampling rate of the data acquisition equipment was 256 samples/cycle or 15360 samples/sec.

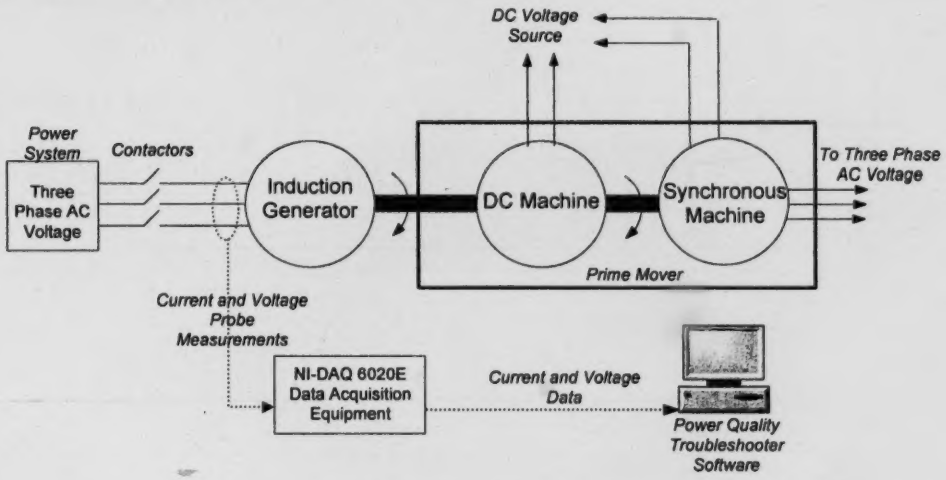

Figure 2.1: Experimental Setup

All experiments were done on the same 3 phase, 4 pole, 7.5 HP,1800RPM, 230V, 60Hz induction machine with modifications to the stator. From the nameplate data, the rated voltage across the stator windings should not exceed 230Vrms. There are three types of stator configurations that are possible:

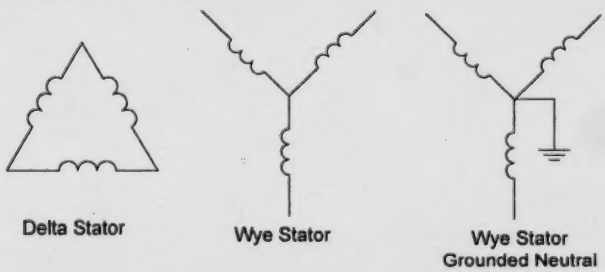

Figure 2.2: Three Possible Stator Configurations

When the machine's stator had a delta connection, a line-line supply voltage of 208V was used. When the machine's stator had a wye connection, a line-line supply voltage of 360V was used.

This ensured that the rated power of the induction machine stayed constant for all the experiments. The full load amps (FLA) of the delta connected machine was 19.6Amps and the FLA of the wye connected machine was 11.3Amps. All experiments were done without the installation of PF correction capacitors.

The purpose of the experiments was to find the largest possible inrush current (maximum peak inrush current) because it can cause the largest possible voltage sag. Using the data acquisition devices, transients similar to the ones shown in Figure 2.3 could be captured.

Figure 2.3 shows a sample transient of the inrush current and the voltage across a contactor before and after it is switched. The moment of switching is at 0.041sec. Prior to 0.041 sec, the contactor is open and no current is flowing. The figure shows that there is a voltage difference across the contactor. At the moment of switching, the contactor is shorted and the voltage instantaneously becomes zero. The current then flows and a peak inrush current correlating with the switching angle is obtained.

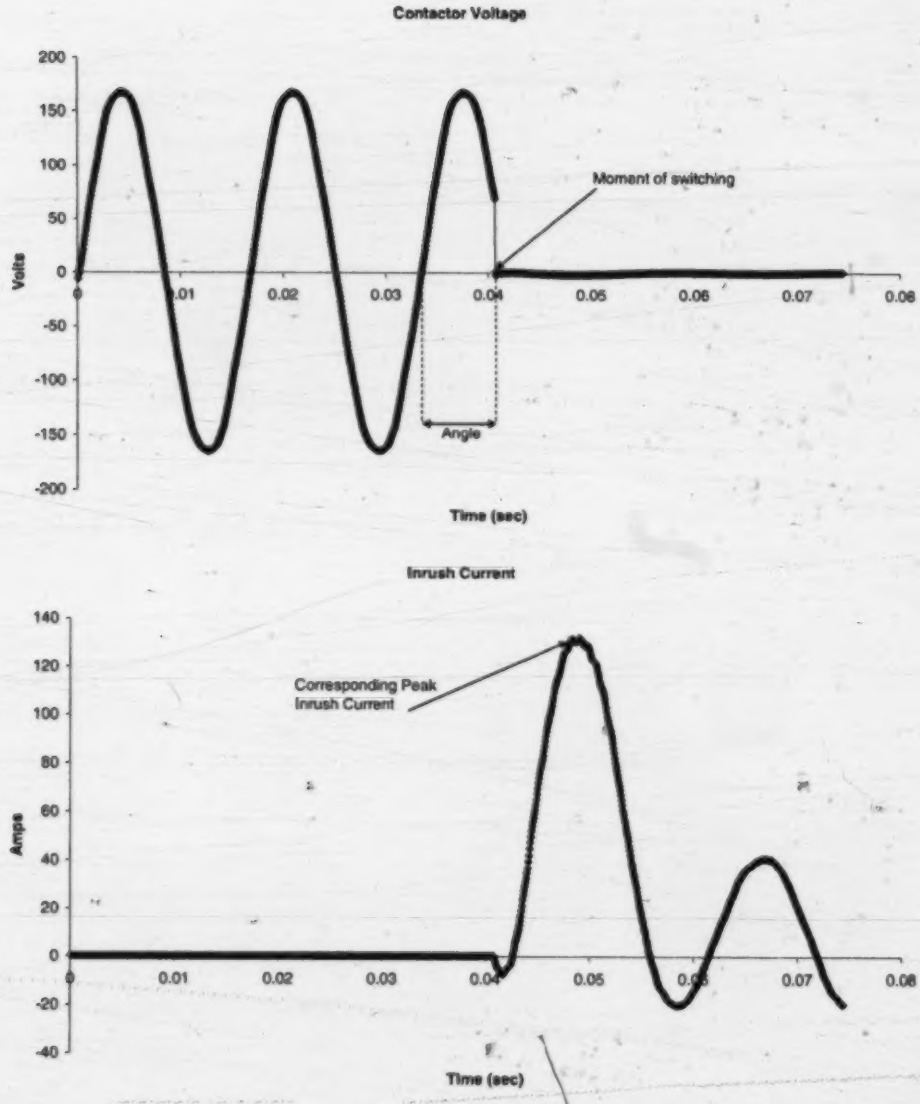

Figure 2.3: Sample Transients

There were two difficulties encountered in the experiments:

1) When connecting the induction machine to the grid at a given rotor speed, the rotor speed did not remain constant. The inrush current caused a transient electromagnetic torque that caused the speed of the rotor to momentarily change. This change in speed, however, was insignificant and was ignored in the analysis. This is because the peak inrush current occurs in the first cycle and so the small change in speed would have a minimal effect on the peak inrush current.

2) The purpose of the experiment was to find the largest possible inrush current (maximum peak inrush current). Obtaining the maximum peak inrush current is difficult because the inrush current varies depending on what moment the contactor is closed. To overcome this difficulty, each switching event was carried out approximately 50 times. A graph of the results was composed, and the maximum peak inrush current was extrapolated.

The inrush current and contactor voltage waveforms were captured approximately 50 times for different stator configurations and varying conditions. A delay was introduced between each switching event to allow the machine speed, terminal voltage, and current to reach steady state prior to the next switching event. Using MATLAB script, the peak inrush current and its corresponding switching angle was extracted from each of the waveforms (see Figure 2.3). The results were then grouped together and plotted against the switching angle of the supply voltage. An example of this is shown in Figure 2.4.

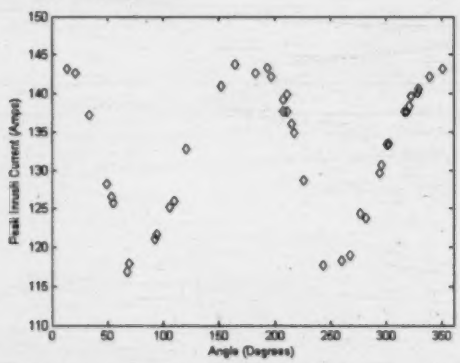

Figure 2.4: Sample Collection of Data

Figure 2.4. demonstrates that the peak inrush current is dependant upon the switching angle. It also allows an extrapolation of the maximum peak inrush current which, in this case, is approximately 143A.

In this section, the experimental setup for all the laboratory experiments was given. Although the switching instant cannot be controlled, the maximum peak inrush current can still be extrapolated by recording the results of 50 switching events.

2.2 Direct Connection

Directly connecting an induction generator to the power grid as shown in Figure 2.5, causes large inrush current that can cause voltage sags to occur.

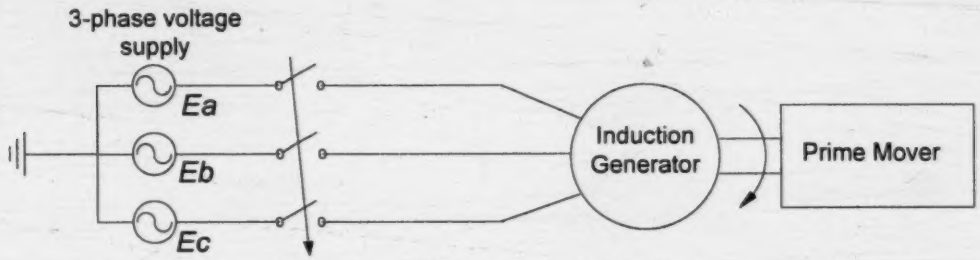

Figure 2.5: Direct Connection Method

The severity of the inrush current depends not only on the switching instant as mentioned before, but also on the speed of the rotor. The transient stator current of an induction generator being connected to a grid at synchronous speed is given in [16] as:

$$I_{a,b,c} = E\left[\frac{1}{X_s} + \left(\frac{1}{X''} - \frac{1}{X_s}\right)e^{(-t/T'')}\right]\cos(\omega t + \lambda) - \frac{E}{X''}\,e^{(-t/Ta)}\cos(\lambda) \qquad (2.1)$$

where :

$X_s = X_m + X_1 + X_t$ = equivalent synchronous reactance

$X'' = X_1 + X_t + \dfrac{X_m X_2}{X_m + X_2}$ = equivalent subtransient reactance

$T'' = \dfrac{1}{\omega R_2}\left(X_2 + \dfrac{X_m(X_1 + X_t)}{X_m + X_1 + X_t}\right)$ = equivalent subtransient short - circuit time constant

$T_a = \dfrac{X''}{\omega(R_1 + R_t)}$ = stator time constant

$\lambda = \lambda_{a,b,c} = \left[\lambda_a + \dfrac{p2\pi}{3}\right]_{p=0,2}$

E = The source phase voltage (rms)

Using the direct connection method, the inrush current was found experimentally for delta, wye, and wye grounded stator configurations. This was done at standstill and at 1800rpm for each configuration. The current in each of the three phases was measured. Since the induction machine is symmetrical, the maximum peak inrush current in all three phases was approximately the same.

Figure 2.6 shows the typical waveforms that would occur in each of the three phases. The duration of the inrush current is longer when the initial rotor speed is 0rpm. The current remains large until the rotor accelerates to a steady state speed of approximately 1795rpm (no-load speed of the induction machine). In Figure 2.6(a), the inrush current duration is short because the rotor is already near 1795rpm.

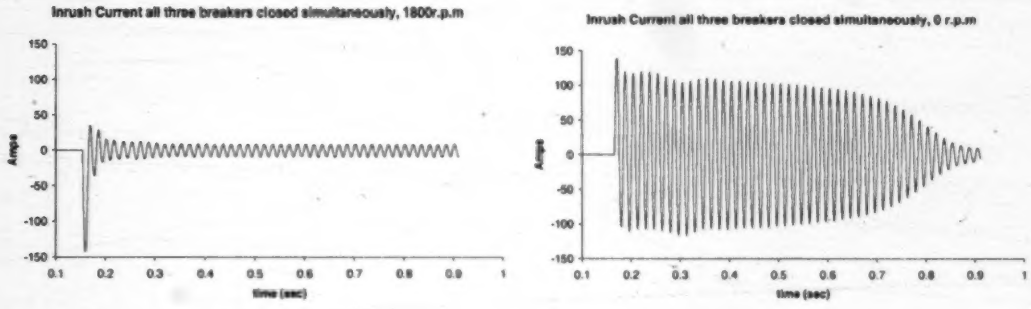

(a) 1800rpm (b) 0rpm

Figure 2.6: Typical Current Waveforms in one of the Phases

Figure 2.7, Figure 2.8 and Figure 2.9 summarize the results obtained when closing the switches 50 times for different stator configurations.

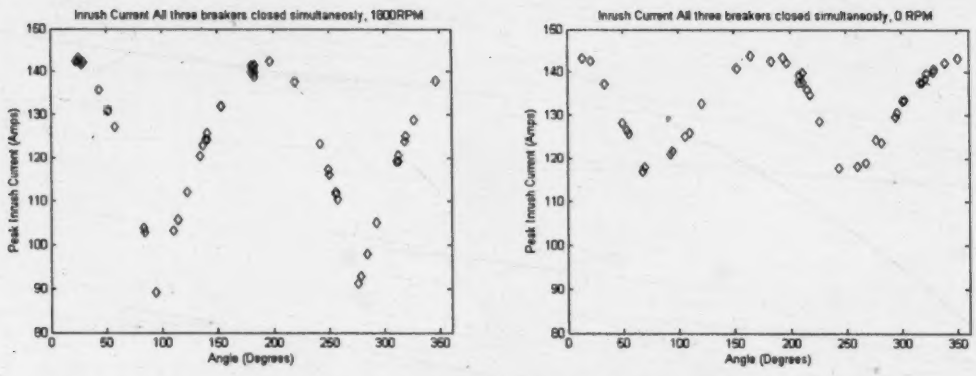
Inrush Current All three breakers closed simultaneosly, 1800RPM
Peak Inrush Current (Amps)
Angle (Degrees)
Inrush Current All three breakers closed simultaneosly, 0 RPM
Peak Inrush Current (Amps)
Angle (Degrees)

Figure 2.7: Direct Connection with Delta Connected Stator

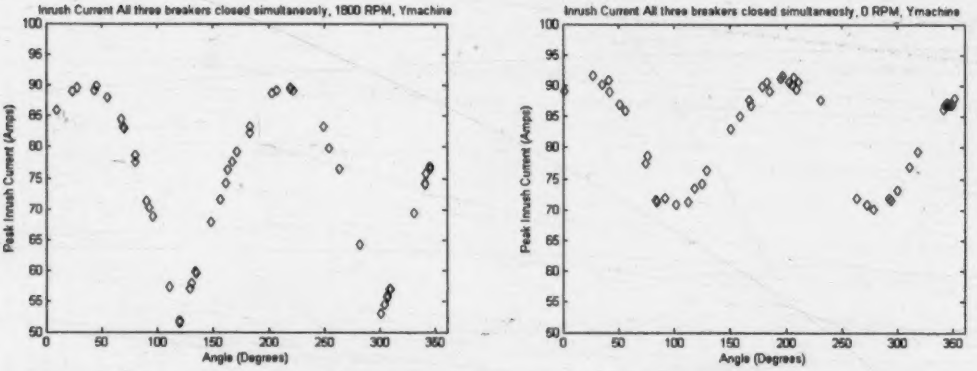
Inrush Current All three breakers closed simultaneosly, 1800 RPM, Ymachine
Peak Inrush Current (Amps)
Angle (Degrees)
Inrush Current All three breakers closed simultaneosly, 0 RPM, Ymachine
Peak Inrush Current (Amps)
Angle (Degrees)

Figure 2.8: Direct Connection with Wye Connected Stator

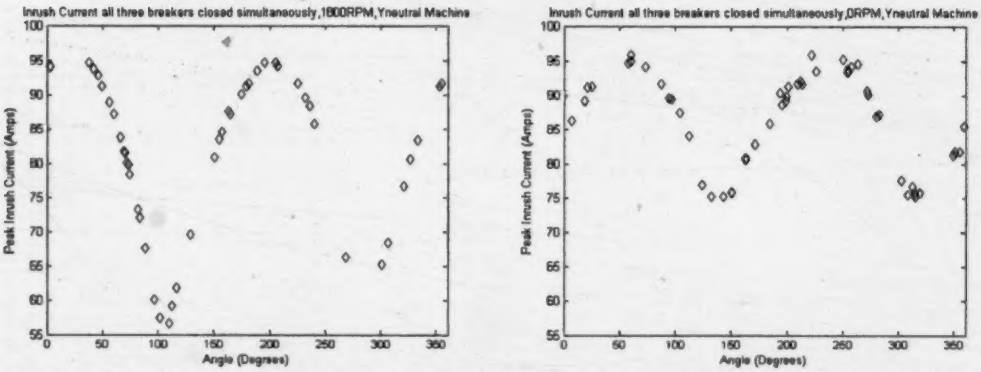
Inrush Current all three breakers closed simultaneously,1800RPM,Yneutral Machine
Peak Inrush Current (Amps)
Angle (Degrees)
Inrush Current all three breakers closed simultaneously,0RPM,Yneutral Machine
Peak Inrush Current (Amps)
Angle (Degrees)

Figure 2.9: Direct Connection with Wye Grounded Connected Stator

The maximum peak inrush current is defined as the largest possible current that can be flowing in the circuit at a specific instant. Connecting the induction generator to the grid 50 times produced

50 data points that were plotted in a graph. Subsequent extrapolation determined the maximum peak inrush current for each configuration. The results are summarized in Table 2.1.

Table 2.1: Summary of Direct Connection

Configuration	Max. Peak Inrush Current	Range	Times larger than FLA
Delta 0rpm	143A	116-143A	516%
Delta 1800rpm	143A	89A-143A	516%
Wye 0rpm	91A	70-91A	570%
Wye 1800rpm	90A	51A-90A	562%
Wye grounded 0rpm	95.9A	75-95.9A	600%
Wye grounded 1800rpm	94A	56A-94A	588%

The minimum peak inrush current is the smallest point in each of the graphs shown in Figure 2.7, Figure 2.8 and Figure 2.9. Depending on the switching instant, the peak inrush current can be anywhere between the maximum peak inrush current and the minimum peak inrush current. Table 2.1 illustrates that a lower peak inrush current can be achieved when connecting at 1800rpm rather than at 0rpm.

The direct connection method results in an inrush current that is much larger than the steady state full load current. The experiments show that the inrush current was 5 to 6 times larger than the FLA. It should be noted again that a supply voltage of 208V was used for the delta connected stator and 360V for the wye connected stator. If the rated machine voltage of 230V for the delta and 400V for the wye connected machine was used, the inrush current would be even larger. It should also be noted that due to the large current during the connection, a very slight and momentary voltage drop occurred at the machine terminals. If the system was perfectly stiff (no system impedance) there would be no voltage drop, and a slightly larger inrush current would occur.

The experiments show that connecting induction machines at synchronous speed and at zero speed will yield the same maximum peak inrush current. However, connecting at synchronous speed allows for a shorter duration of inrush current and thus, a shorter duration of voltage sag. This translates to a softer grid connection.

2.3 Three Series Resistor Method

The three series resistor method is an effective way of connecting induction generators and motors to the grid while minimizing inrush current. In the laboratory experiment, an induction machine was connected to the grid at a rotor speed of 1800rpm using this method. The connection procedure consisted of two steps. The first step was to close contactors A, B and C simultaneously while the rotor was spinning at 1800rpm. This is shown in Figure 2.10.

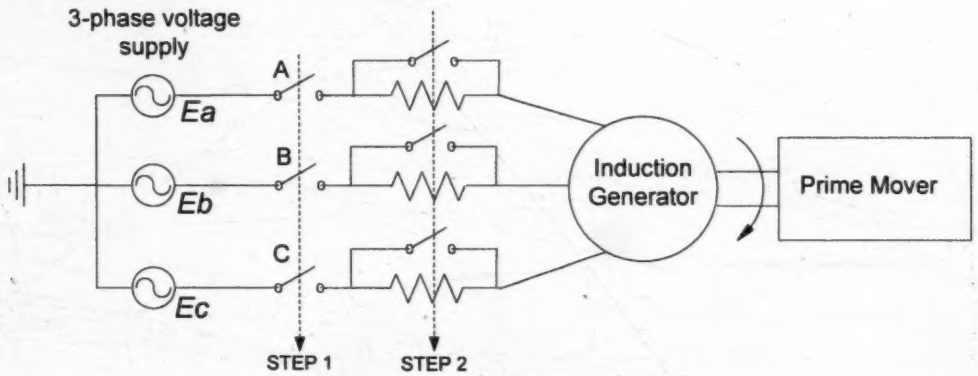

Figure 2.10: Three Series Resistor Method

The second step of the connection procedure was to bypass all three resistors simultaneously. This step was executed when the induction machine currents reached a steady state value. Both step one and step two will yield inrush current since there were no PF correction capacitors installed. The larger the resistor size, the smaller the step one inrush current will be. However, the larger the resistance value is, the larger the step two inrush current will be.

This experiment was done on two different stator configurations. 1) Delta connected stator and 2) Wye connected stator. The wye grounded neutral stator configuration was omitted because the machine was balanced and so the results would be almost identical with the ungrounded wye connected stator configuration. The resistance value in each phase was the same.

The purpose of this experiment was to obtain the optimal resistor size that would best minimize the inrush current of the induction machine. In order to find this optimal resistor size, the switching was done approximately 50 times for varying resistances. The inrush current in each of the phases was captured by the LABView data acquisition equipment. The peak inrush current

from each of the 50 current waveforms was extracted and the largest value (maximum peak inrush current) in this group was plotted versus resistance in Figure 2.11 and Figure 2.12. The maximum peak inrush current obtained was the same in each of the three phases because the induction machine and the voltage supply were balanced and the resistance values in each phase, the same.

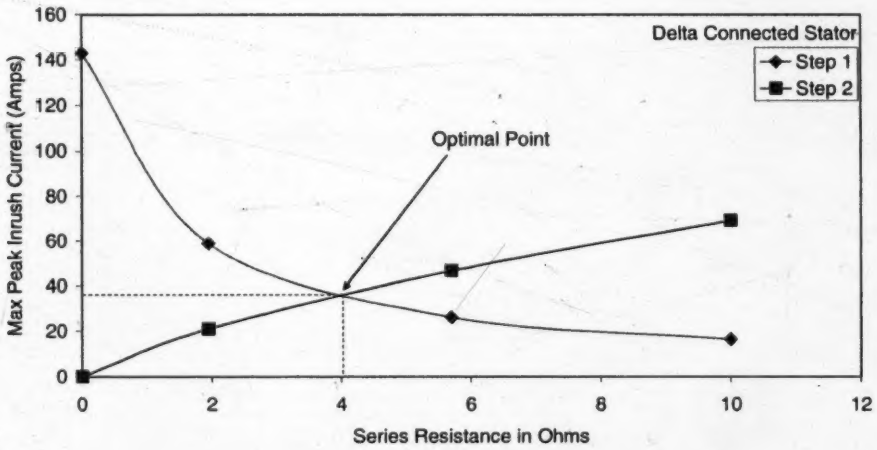

Figure 2.11: Inrush Current Curves for Delta Connected Stator

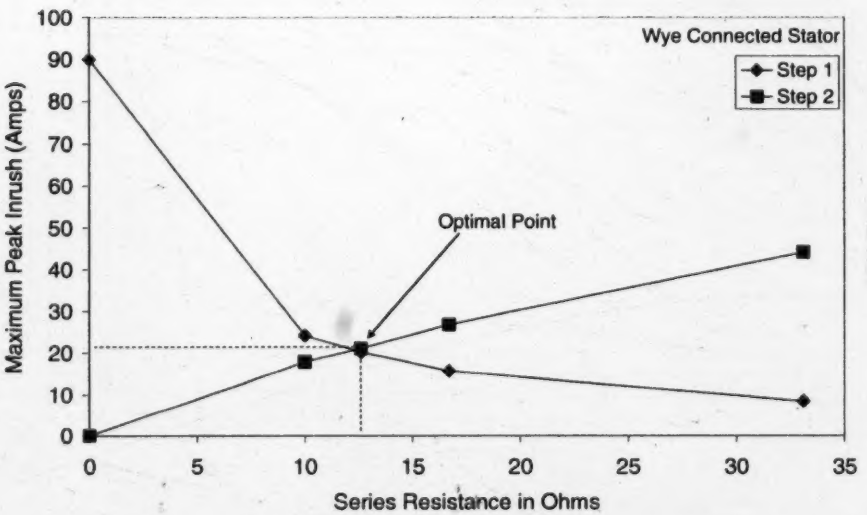

Figure 2.12: Inrush Current Curves for Wye Connected Stator

Both optimization curves exhibit similar curve patterns. As the series resistor size increases, the step one inrush current decreases. This is expected, since the series resistor adds additional resistance to the induction machine. However, the larger the resistor, the larger the inrush current was when the resistors were bypassed in step two. The optimal point occurs where the step one and step two curves intersect. Inserting a 4Ω resistor in each phase of the delta connected stator reduced the inrush current from 143A peak to 37A peak. Similarly, inserting a 12.2Ω resistor in each phase of the wye connected stator reduced inrush current from 90A peak to 21A peak. This method is effective in reducing inrush current and is more cost effective than using a thyristor controlled soft-starter.

Table 2.2: Three Series Resistor Summary

Stator Configuration	Optimal Resistance Value	Max Peak Inrush (Amps)	Percent Reduction compared to Direct connection
Delta Connected	4Ω	37A	74%
Wye Connected	12.2Ω	21A	76%

2.4 Summary

In this chapter the equipment used to determine the inrush current was described. The purpose of the experiments was to determine the largest (maximum) peak inrush current that can occur when connecting an induction generator using different methods. The largest current will yield the largest voltage sag, thus, the worst case scenario was considered. The peak inrush current varies depending on the moment of switching. Consequently, numerous switching events were recorded in order to find the maximum peak inrush current.

This chapter also shows the experimental results when connecting an induction generator directly to the grid. It was found that the value of the maximum peak inrush current is not dependant on the rotor speed. However, the *duration* of the inrush current is dependent on the rotor speed, with duration decreasing as rotor speed approaches synchronous speed. Minimization of the duration of inrush current will result in minimization of voltage sag. Therefore, connecting the induction generator to the grid at around synchronous speed reduces the duration of the inrush current.

One method to reduce the inrush current that occurs when connecting an induction generator is to use the three series resistor method. Experimental results showed that this method can reduce inrush current by approximately 75%.

The three series resistor method requires 3 resistors and 3 bypassing contactors. Since a malfunction in any one part of the system leads to failure, systems operating with numerous parts are at greater risk of failure. Additionally, systems with multiple parts have higher start-up costs. In the next chapter, a more cost effective and reliable method of reducing inrush current will be investigated.

Chapter 3

Experimental Study of the Proposed Methods

A total of four experiments were conducted on the proposed methods described in section 1.4. The experimental results are presented in this chapter. The first experiments involve the scheme of using a single series resistor to limit inrush current. Three generator configurations, namely delta, wye, and wye grounded, were studied. The fourth experimental study involves the scheme of using a neutral resistor. This scheme can only be used on a wye grounded generator.

3.1 Introduction

The proposed methods call for sequential closing of contactors. As a result, each of the four generator configurations require multiple steps of switching before they are fully connected to the grid. Each step was tested for different resistance values so that the effect of the single resistor could be determined. When a switch is closed, inrush current could potentially occur in all phases that are energized. In other words, the peak inrush current does not necessarily occur in the phase that was switched. Consequently, more than one current probe was required to capture the peak inrush current in each energized phase. The peak inrush current for each step was captured approximately 50 times. A delay between each captured switching event was necessary to ensure the machine voltages and currents would reach steady state prior to the next switching event. The 50 peak inrush current values were then plotted versus the switching angle so that the maximum peak inrush current value could be obtained. The maximum peak value was extracted using MATLAB script. The maximum peak in each step was then plotted versus the resistance. Based on these plots, the resistor value that best minimized the inrush current was extrapolated. The

effectiveness of the two new methods was evaluated by comparing the inrush current with the direct connection method and the three series resistor method.

3.2 Single Series Resistor Method

The single series resistor method was tested on three different generator configurations: delta, wye, and wye grounded. A single series resistor was placed between one of the stator terminals and one of the voltage source terminals. By sequentially connecting each of the phases in steps, the inrush current for each configuration was minimized. Also included in the procedure was a step that bypassed the resistor. The delta and wye configurations required only three steps to be normally connected to the grid. The wye neutral grounded connection required four steps. The first sub-section shows the experimental results when connecting the delta configured generator. The delta configuration was tested at different rotor speeds and the results are described in steps. The wye and wye neutral grounded configured generators were connected to the grid using the proposed method at a constant rotor speed of 1800rpm. This method can be used with a single series resistor place in phase A, B or C. It was arbitrarily chosen to place the resistor in phase C for all three configurations. If the resistor was placed in phase A or B, the switching sequences would be different, but the results would be similar.

3.2.1 Delta Configuration

Using this configuration, three terminals need to be connected to the grid, and a resistor needs to be bypassed. An overview of the experimental setup is shown in Table 3.1 and Figure 3.1. The experiments were conducted using the following line-ground rms voltages:

$$Ea = 120\angle 0^{\circ},\ Eb = 120\angle +120^{\circ},\ Ec = 120\angle -120^{\circ}$$

Figure 3.1 shows that 4 contactors must be closed in order to fully and normally connect the generator to the grid without the resistor. There are four different sequences in which this can be done (see Table 3.1).

Table 3.1: Delta Configuration

Possible Sequences

Sequence	STEP 1	STEP2	STEP 3
CBAR	C and B	A	R
CBRA	C and B	R	A
CABR	C and A	B	R
CARB	C and A	R	B

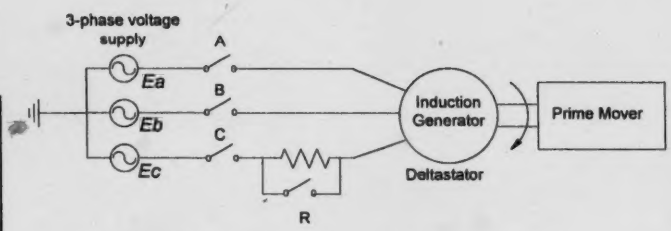

Figure 3.1: Delta Configuration

From the experimental setup shown, the following conclusions can be made:

- No current will flow until C and either A or B are closed.
- Step one of all four sequences will have the same inrush current since the impedance across any two voltage terminals will be the same.
- Sequence CBRA and CARB will yield similar inrush current results since the electric circuit prior to each step is identical.

From the previous observations, the first step requires the closure of two circuit breakers. Since sequence CBRA and CARB are identical, only three sequences were tested. The inrush current results have been divided into steps.

Step One

The magnitude of the voltage across any two lines was 208Vrms, since the voltage source was balanced. This voltage is the fixed supply voltage and is therefore not dependant on the speed of the induction generator. The experiments show that the maximum peak inrush current in step one is not dependant on speed either. The maximum peak inrush current is plotted versus the series resistor value in Figure 3.2.

Figure 3.2 shows that the maximum peak inrush current decreases as the series resistor size increases. This is because the resistor effectively increases the impedance between the source voltages. Closing C & A or closing C & B in the first step yields the same results, as expected. This is because the electric circuit is the same for both cases. The results show that the maximum peak inrush current in step one is independent of sequence and rotor speed.

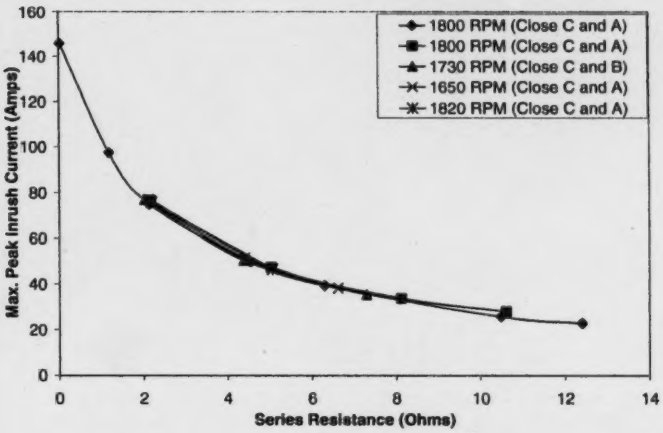

Figure 3.2: Max. Peak Inrush Current in Step One

When executing step one at lower rotor speeds, the machine will help accelerate the rotor to synchronous speed. Since generation only occurs when the rotor is above synchronous speed, this acceleration allows power generation to occur more quickly. However, the lower the rotor speed is at the moment of connection, the longer the duration of the inrush current. As shown in Figure 3.3, the duration of the inrush current when connecting at 1640rpm lasted longer than at 1800rpm. At 1640rpm, the machine draws large current until the rotor accelerates to a no-load speed of approximately 1800rpm. Connecting at 1800rpm does not require any acceleration and therefore does not draw large current from the grid for as long.

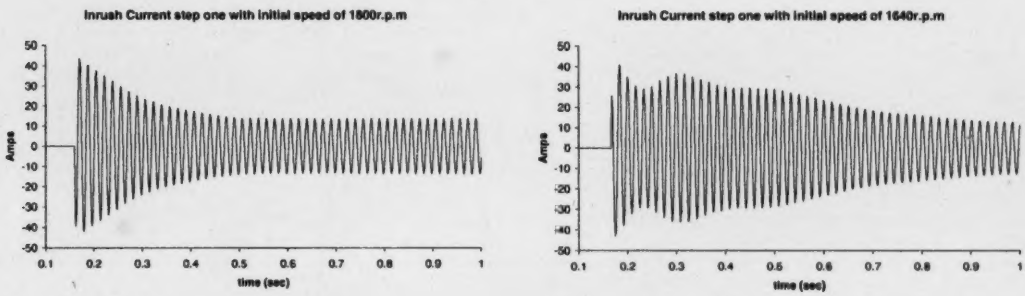
Inrush Current step one with initial speed of 1800r.p.m
Amps
time (sec)
Inrush Current step one with initial speed of 1640r.p.m
Amps
time (sec)

Figure 3.3: Inrush Current at Different Rotor Speeds in Step One, R=4.76Ω

It was observed that a minimum speed requirement must be achieved before the first step was executed. This speed in our experiment was around 1600rpm, and is larger for larger series resistor values. When the minimum speed requirement was not met, the electromagnetic torque

was not large enough to accelerate the machine further. As a result, the inrush current would persist and would cause the machine to overheat if it was not disconnected. The duration of the inrush current was the smallest for speeds of 1795, 1800 and 1810rpm. For each of these speeds, the inrush current duration was approximately the same because the prime mover was providing the power and there was no need for the machine to draw current to accelerate the rotor further. The step one results are summarized below:

- Regardless of speed, the maximum peak inrush current decreases as the resistance increases.
- The step one maximum peak inrush current is independent of rotor speed and sequence.
- The speed of the rotor only effects the duration of the inrush current and does not affect the maximum peak inrush current.

Step Two

According to Table 3.1, there are three possible connections that can occur: close A, B or R. Closing R in sequence CBRA or CARB will yield the same inrush current results. Testing CARB would be redundant, so the sequence was omitted. From the experimental results, the maximum peak inrush current that occurred in step two was dependent on 3 things: the speed of the rotor, the series resistor value and the selected contactor that was closed.

Figure 3.4 shows the maximum peak inrush current versus series resistance. Unlike step one, the inrush current was dependant on the rotor speed and the sequence number. The step one inrush current is also shown in each chart as a reference. The experiment was done at three constant rotor speeds (1795rpm, 1800rpm and 1810rpm). The switching event that occurs is also shown next to the chart.

It should be noted that at the moment of switching, the speed of the rotor varied between 1792 and 1796rpm. This was because the DC machine controller was unable to maintain a constant rotor speed of exactly 1795rpm. For 1800rpm and 1810rpm the prime mover remained connected and was able to maintain the rotor speed at 1800rpm and 1810rpm respectively.

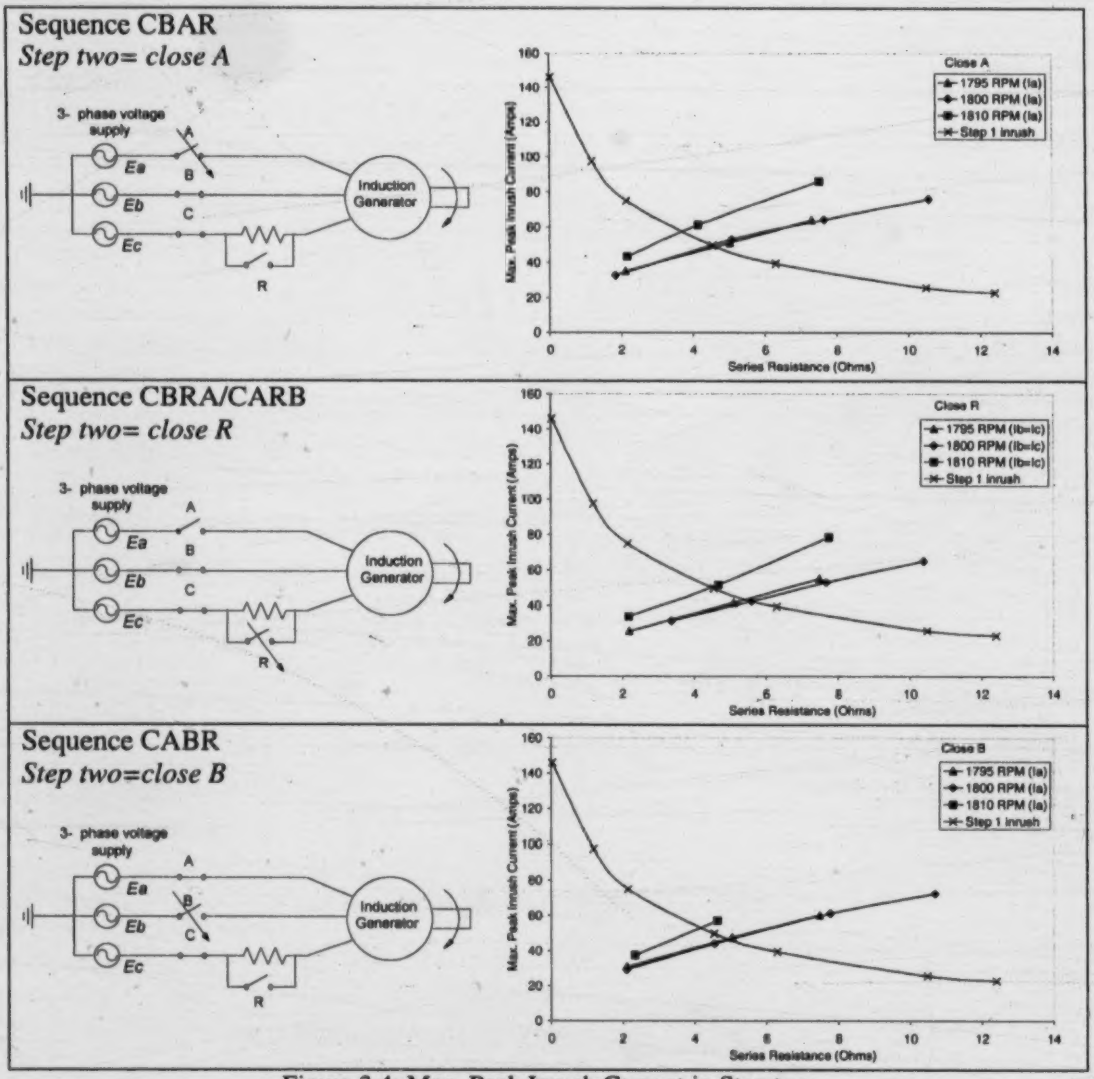

Figure 3.4: Max. Peak Inrush Current in Step two

The step two results are summarized below:

- The inrush current is proportional to the series resistor value in the tested range and increased as the resistor size increased.
- The peak inrush current at 1795 and 1800rpm was approximately the same.
- The peak inrush current at 1810rpm yielded the highest inrush current.

Step Three

According to Table 3.1 there are three possible events that may take place: close A, B or R. The contactor that is closed in step three depends on which sequence was chosen. For sequence CBAR and CABR, R is closed in step three. The circuit for these 2 sequences prior to step 3 are exactly the same, as shown in Figure 3.5. Since the resistor is still part of the circuit, the inrush current that occurs when the resistor is bypassed depends on the resistor size. The larger the resistor, the larger the inrush current. Figure 3.5 also illustrates that the inrush current is dependent on the rotor speed. At 1810rpm, the inrush current is larger than at 1800rpm and at 1795rpm.

Sequence CBAR/CABR

Step 3= close R

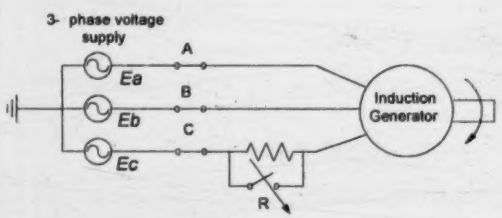

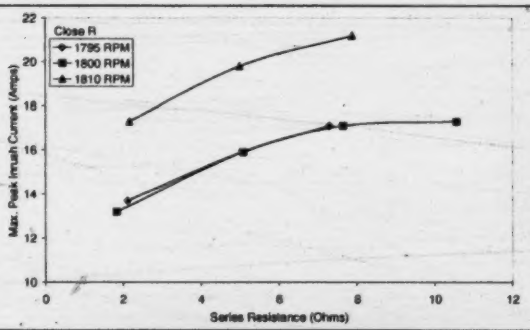

Sequence CARB

Step 3= close B

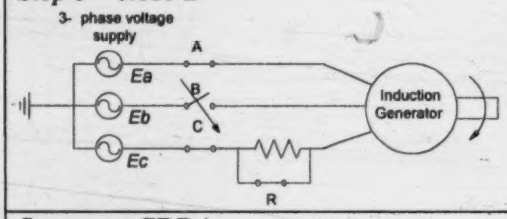

Max Peak Inrush Current	Rotor Speed
19.45A	1795rpm
20.3A	1800rpm
26.1	1810rpm

Sequence CBRA

Step 3=close A

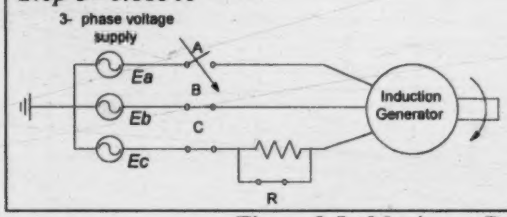

Max Peak Inrush Current	Rotor Speed
21.7A	1795rpm
22A	1800rpm
27.4A	1810rpm

Figure 3.5: Maximum Peak Inrush Current in Step Three

For sequence CARB and CBRA, the resistor was bypassed in step two, so the resistor was no longer part of the circuit. As a result, the inrush current that occurs in step three is independent of the resistor size. The results also show that the inrush current is dependant on the speed of the rotor. At 1810rpm, the inrush current was the largest. Since the circuits for sequence CARB and CBRA are similar, the peak inrush currents are approximately the same. Some asymmetry in the stator windings leads to a slight difference in results between the two sequences.

The most important finding obtained from the step three experiments is that the inrush current is much smaller than the step one and two inrush currents. Therefore, only the step one and two results are required in determining the optimal resistance value, since the step three inrush current is negligible.

3.2.2 Delta Configuration Summary

The step one inrush current decreases as the resistor value increases, but the step two inrush current increases as the resistor value increases. The optimal point (regardless of the speed) is the intersection of the step one and two inrush current curves. The optimal point is independent of the step three inrush current since it is so small. The data from each sequence has been plotted together, and an optimum point has been obtained. Figure 3.6 shows the optimal point for each sequence when the rotor speed was 1800rpm.

From Figure 3.6 the sequence that produces the lowest inrush current is sequence CBRA/CARB. The intersection of the step one inrush current and step two inrush current is approximately (5.6,42.7). In other words, the series resistor value that minimizes the inrush current to 42.7A is 5.6Ω. The step three curve for sequence CBRA/CARB is a flat line since the resistor was bypassed in step two and is not dependant on the resistor size.

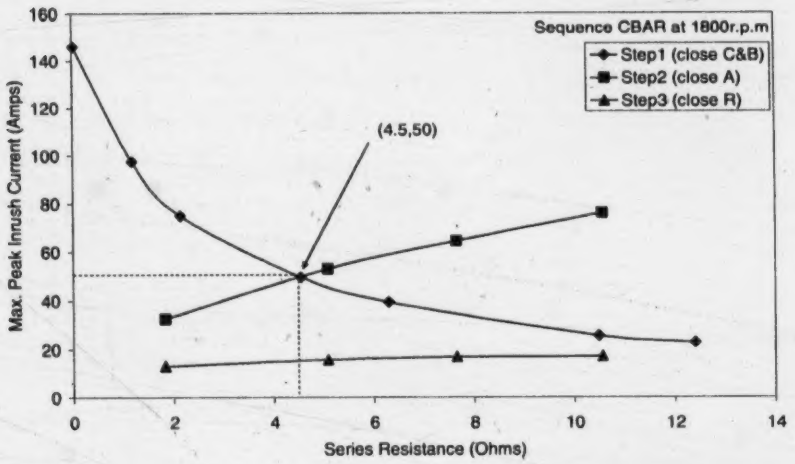

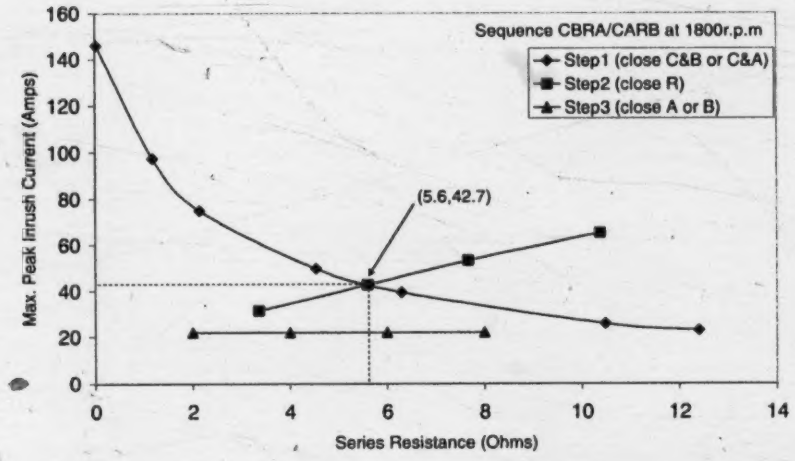

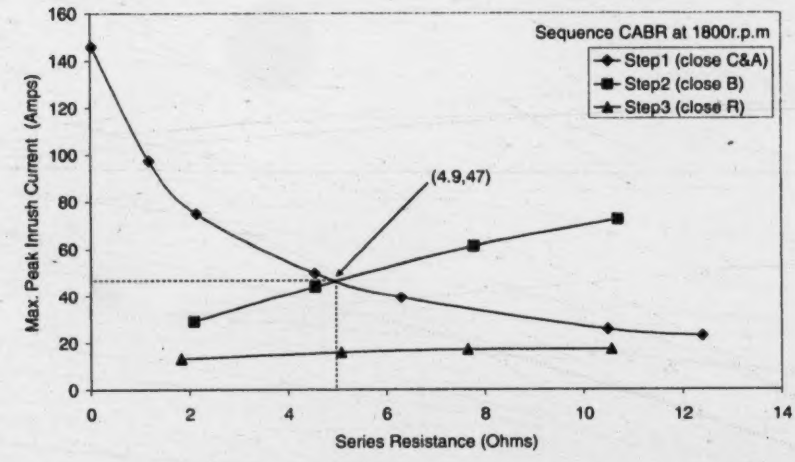

Figure 3.6: Series Resistor Inrush Current Curves 1800rpm (Delta Configuration)

Similarly we can get the optimal point for the sequences at rotor speeds of 1795rpm and 1810rpm. Figure 3.7 is a collection of the inrush currents at the optimal point for the tested rotor speeds and sequences.

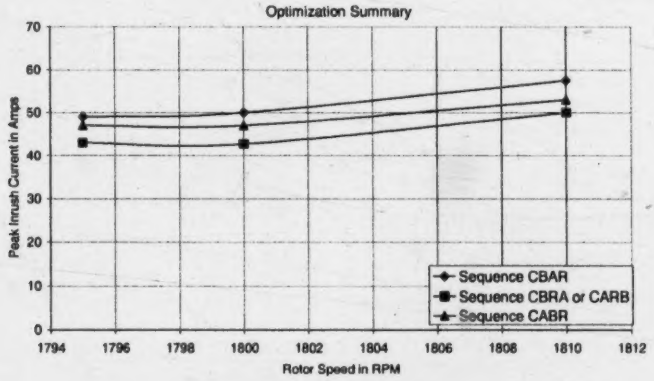

Figure 3.7: Optimization Summary

The inrush current is approximately the same for rotor speeds of 1795rpm and 1800rpm. However, a rotor speed of 1810rpm yields the highest inrush current for all sequences. From Figure 3.7 it is shown that sequence CBRA/CARB is best for minimizing inrush current for all the tested rotor speeds. For each sequence, an optimal resistor is selected such that the inrush current can be minimized. However, as the speed of the rotor changes, so does the optimal resistor size. This is demonstrated in Figure 3.8.

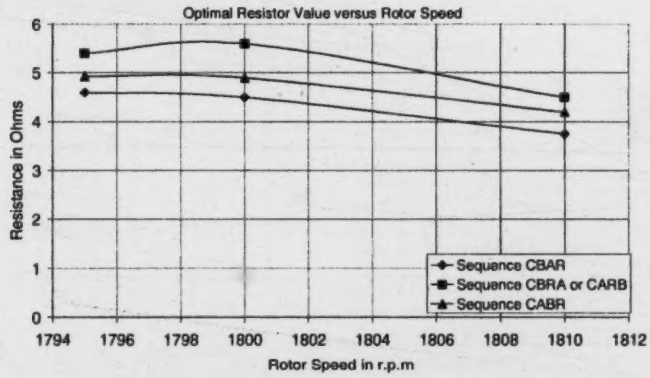

Figure 3.8: Optimal Resistance Value

Using a single series resistor to connect an induction generator with a delta configuration to the grid is effective. From laboratory experiments it was determined that the most effective rotor

speed for connection is approximately synchronous speed. This speed has 2 advantages: 1) yields the shortest duration of inrush current during the first step and 2) minimizes the maximum peak inrush current in the second step.

The important conclusions are listed below.

- The best sequence at any speed is either sequence CBRA/CARB. These two sequences will yield the same inrush currents since they both bypass the resistor in the second step.
- The intersection point of the step one and two inrush current curves define the optimal resistor that will best minimize the inrush current.
- Step three inrush current is small and does not effect the optimal resistor size selection.
- Using sequence CBRA/CARB, connected at a rotor speed of 1800rpm, yields a maximum peak inrush current of only 42.7 A. This is a 70% reduction in inrush current compared to the direct connection method. The resistance required to achieve this was approximately 5.6Ω.
- The optimal resistance value R is specific to each rotor speed. In order to optimize inrush current minimization, the induction generator should be run at a rotor speed that corresponds to the optimal resistance value. For example, the optimum resistance value for sequence CBRA/CARB, running at 1800rpm was 5.6Ω. If this resistor size was used for connecting at a rotor speed of 1810rpm, the peak inrush current would be approximately 60A rather than 42.7A. This is a significant increase in inrush current and as a result, careful control is required during the connection procedure to ensure that the desired rotor speed is acquired.

3.2.3 Wye Configuration

In this experiment, the inrush current was only measured at a single rotor speed of 1800rpm. This is because in the previous section, it was found that the inrush current trends did not change at different rotor speeds. Also, it was difficult to obtain constant speeds of 1795 and 1810rpm in the experiments with the DC machine as the prime mover. Using the synchronous machine as the prime mover with a rotor speed of 1800rpm proved to be much easier. In order to be efficient in obtaining results, it was decided to test all remaining configurations at a single rotor speed of 1800rpm.

Using the wye configuration, three terminals need to be connected to the grid and one resistor needs to be bypassed. An overview of the experimental setup is shown in Figure 3.9. The experiments were conducted using the following line-ground rms voltages:

$$Ea = 208\angle 0^{\circ},\ Eb = 208\angle +120^{\circ},\ Ec = 208\angle -120^{\circ}$$

From Figure 3.9, 4 contactors must be closed in order to fully and normally connect the generator to the grid without the resistor. There are four different sequences in which this can be done (see Table 3.2).

Table 3.2: Wye Configuration

Possible Sequences

Sequence	STEP 1	STEP2	STEP 3
CBAR	C and B	A	R
CBRA	C and B	R	A
CABR	C and A	B	R
CARB	C and A	R	B

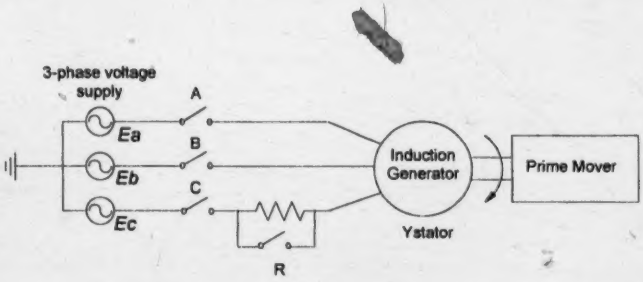

Figure 3.9: Wye Configuration

From the experimental setup shown in Figure 3.9 the following conclusions can be made:

- No current will flow until C and either A or B are closed.
- Step one of all four sequences will have the same inrush current since the impedance across any two voltage terminals will be the same.
- Sequence CBRA/CARB will yield similar inrush current results since the electric circuit prior to each step is identical. As a result, CARB was not tested.

A detailed description and discussion of the experiment is given in the previous section. To avoid repetition, only the main results will be shown and discussed in this section. The inrush current curves for each sequence are shown in Figure 3.10.

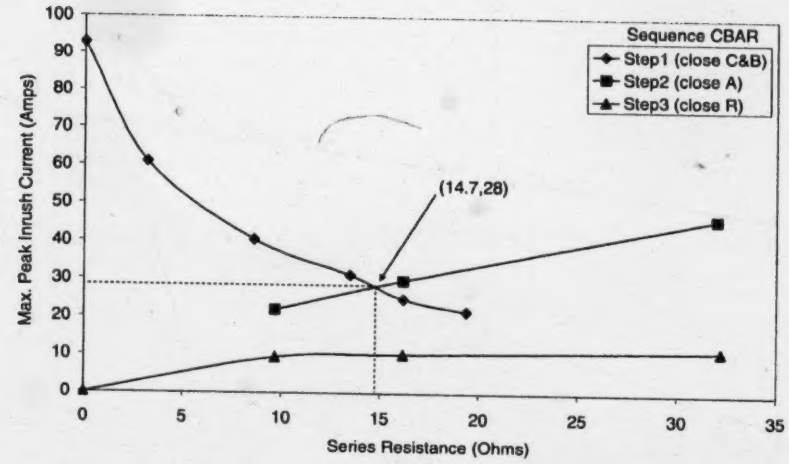

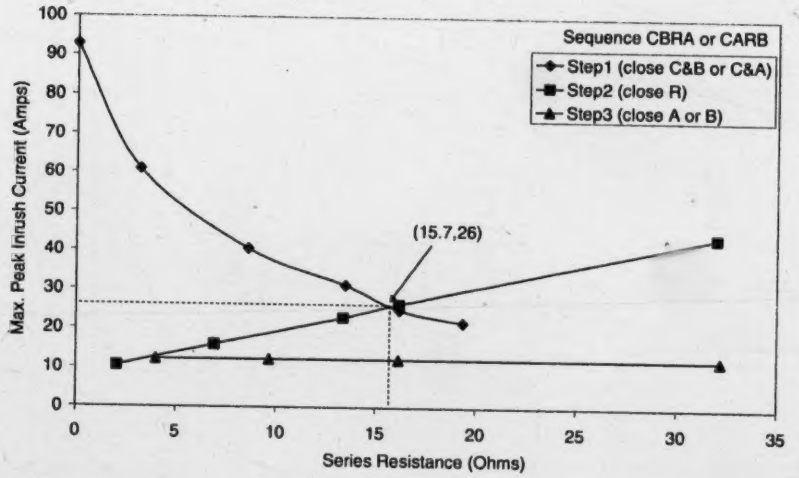

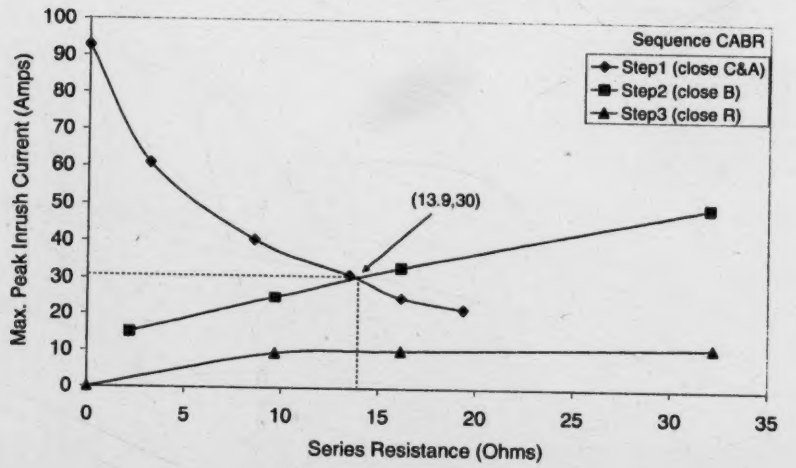

Figure 3.10: Series Resistor Inrush Current Curves at 1800rpm (Wye Configuration)

An optimal point can be extracted from each graph. Below is a list of points that summarize the experimental results.

- For each sequence, step one and two determine the optimal resistor size and the minimum current that can be obtained. The intersection of the two curves is the optimal point. The step three inrush current is comparatively small and does not affect the optimal resistor size.
- The sequences that best minimize the inrush current are sequences CBRA/CARB. Both of these sequences bypass the resistor in step two. The step three inrush current is represented as a straight line in Figure 3.10 because it is independent of the bypassed resistor.
- The optimal resistor size for sequence CBRA/CARB is approximately 15.7Ω, and the maximum peak inrush current at this resistance value is 26Amps.

This new method of reducing inrush current in a wye configured induction generator works effectively. The CBRA/CARB sequences running at 1800rpm gave a maximum inrush current of 26A peak. This is a 71% reduction compared to the 90A peak when connecting directly. CBRA/CARB consist of first closing two contactors such that the inrush current is limited by the resistor. The next step is to bypass the resistor and the last step is to close the remaining contactor. Like the delta configuration experiments, the step three inrush current does not effect the optimal resistor size. This is because the inrush current is small compared to the step one and two inrush currents. Although the experiment was only conducted at 1800rpm, it is likely that similar inrush current curves would be seen at rotor speeds of 1795 and 1810rpm.

3.2.4 Wye Grounded Configuration

The single series resistor method can also be utilized on a wye grounded stator configuration. Unlike the ungrounded configurations discussed thus far, this machine's configuration is such that it will draw current after closing one contactor in the first step. This gives 6 different possible sequences to be tested (see Table 3.3). Since there are three terminals and one resistor, there are a total of 4 contactors that need to be closed as shown in Figure 3.11. As mentioned in the previous section, it is suitable to conduct the experiments at a single rotor speed of 1800rpm. The experiments were conducted using the following line-ground rms voltages:

$$Ea = 208\angle 0^{\circ},\ Eb = 208\angle +120^{\circ},\ Ec = 208\angle -120^{\circ}$$

Table 3.3: Wye Grounded Configuration

Possible Sequences

Sequence	STEP 1	STEP2	STEP 3	STEP4
CBAR	C	B	A	R
CBRA	C	B	R	A
CABR	C	A	B	R
CARB	C	A	R	B
CRBA	C	R	B	A
CRAB	C	R	A	B

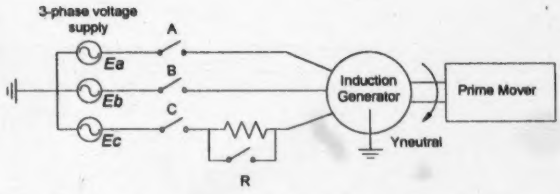

Figure 3.11: Wye Grounded Configuration

In this experiment, step one and step two yield the largest inrush current. The first step is to close the phase which contains the resistor (close phase C). There are three possibilities for step two. They are: close phase B, close phase A or bypass the resistor. Below is a graph that summarizes the results from steps one and two.

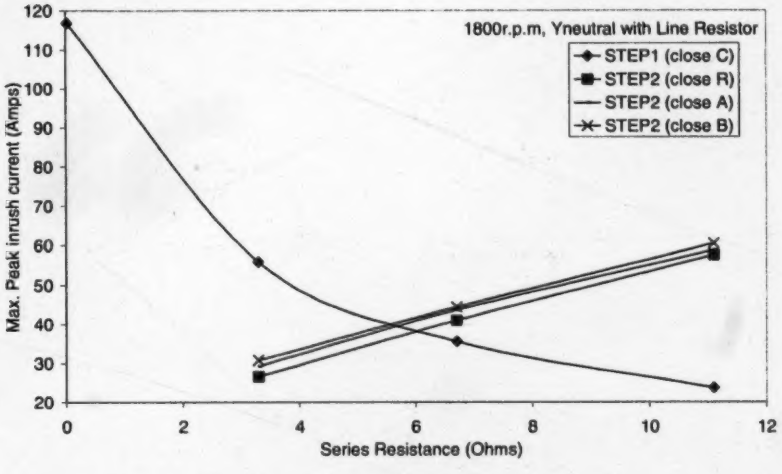

Figure 3.12: Step One and Two Peak Inrush Current Curves

Figure 3.12 shows that closing R in step two results in the lowest peak inrush current. Therefore the sequences that best minimize the inrush current are the sequences that bypass R in the second step: CRBA, CRAB. The other sequences do not need to be tested because they will not allow us to achieve an inrush current as low as the CRBA, CRAB sequences.

For sequence CRBA and CRAB step three should involve closing B or closing A. If B is closed in step three, the peak inrush current is 18.8A. If A is closed in step three, the peak inrush current

is 15.9A. In step four the final contactor is closed. This is either A or B. From the experimental results, the inrush current measured when closing A, was 9Amps for sequence CRBA and when closing B, was 9.8Amps for CRAB. This slight difference can be due to slight asymmetry in the motor windings.

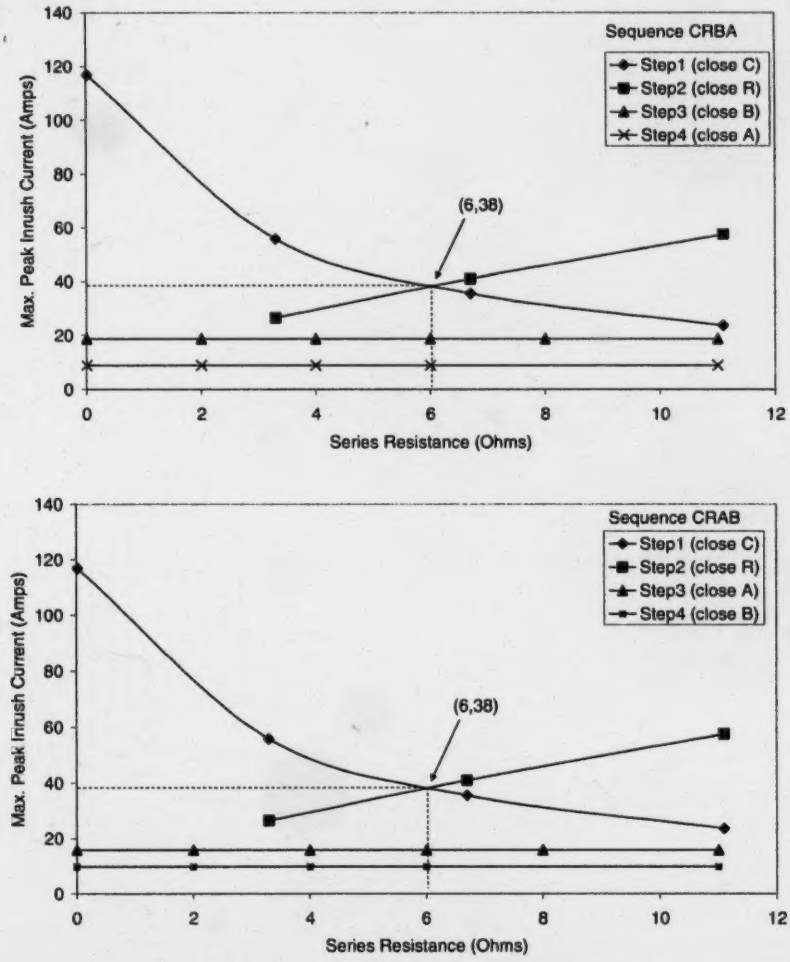

Figure 3.13: Sequence CRBA and CRAB Inrush Current Curves (Wye Grounded Config.)

From Figure 3.13, the step 1 inrush current decreases as the resistance size increases and the step 2 inrush current increases as the resistance value increases. The intersection of these two curves is the optimal point. The optimal point on the graphs occur when the resistor size is approximately 6Ω and the resulting peak inrush current is 38A. Step three and four inrush currents are much

smaller than the step one and two inrush current and are not dependent on the bypassed resistance value. As a result, they do not effect the optimal point. The step three inrush current for sequence CRAB is smaller than for sequence CRBA. Equal inrush currents are expected when step four is carried out.

The CRBA and CRAB sequences, running at 1800rpm, gave a peak inrush current of 38A. Compared to the 94A peak of the direct connection method, this is a 60% reduction. This shows that this method is quite effective in reducing the inrush current of an induction generator with a wye grounded configuration. Only the CR sequences needed to be tested in order to find the optimal resistor that minimized inrush current. This reduced the number of experiments that were required.

3.3 Neutral Resistor Method

The neutral resistor method can only be utilized on a generator with a wye grounded stator configuration. The current limiting resistor was placed between the common point of the wye stator and ground. The experiments were conducted at a single rotor speed of 1800rpm. There are several different sequences in which the induction generator can be gradually connected to the grid. There are four steps required since there are four switches that need to be closed independently. This gives 6 different combinations that would need to be tested (see Table 2.1). The experiments were conducted using the following line-ground rms voltages:

$$Ea = 208\angle 0^{\circ},\ Eb = 208\angle +120^{\circ},\ Ec = 208\angle -120^{\circ}$$

Table 3.4: Neutral Resistor Method Possible Sequences

Sequence	STEP 1	STEP2	STEP 3	STEP4
ABCR	A	B	C	R
ABRC	A	B	R	C
ACBR	A	C	B	R
ACRB	A	C	R	B
ARBC	A	R	B	C
ARCB	A	R	C	B

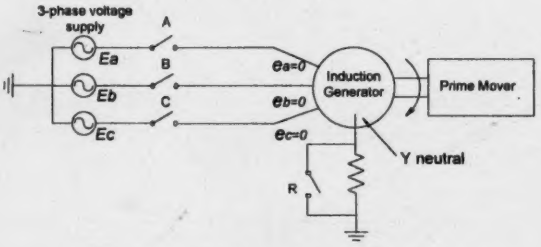

Figure 3.14: Neutral Resistor Method

The first step of this method is to close one of the phases. The electric circuit of phase A, B and C are identical. As a result, the same inrush current would be seen regardless of which phase was closed first. In this experiment, phase A was arbitrarily chosen to be the first phase closed. There are 3 possibilities for step two: close B, close C, or bypass the resistor. Steps one and two result in the most severe inrush currents, and a graph with this data is summarized in Figure 3.15.

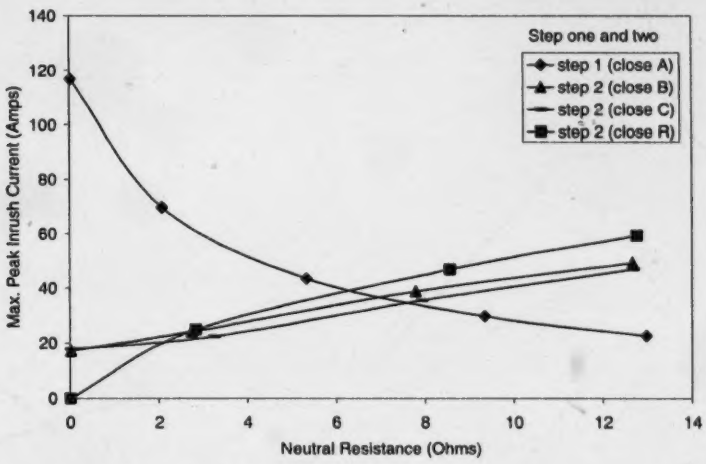

Figure 3.15: Summary of Step One and Two Inrush Current (Neutral Resistor Method)

Figure 3.15 illustrates that as the resistor value increases, step one inrush current decreases and step two inrush current increases. It also shows that for all resistance values greater than 3Ω, closing C in step two yielded the smallest inrush current. Therefore, the sequences that best minimize the inrush current are sequences that close C in step two: ACBR, ACRB. The other sequences do not need to be tested because they will not allow us to achieve an inrush current as low as the AC sequences. The inrush current for the AC sequences are shown in Figure 3.16.

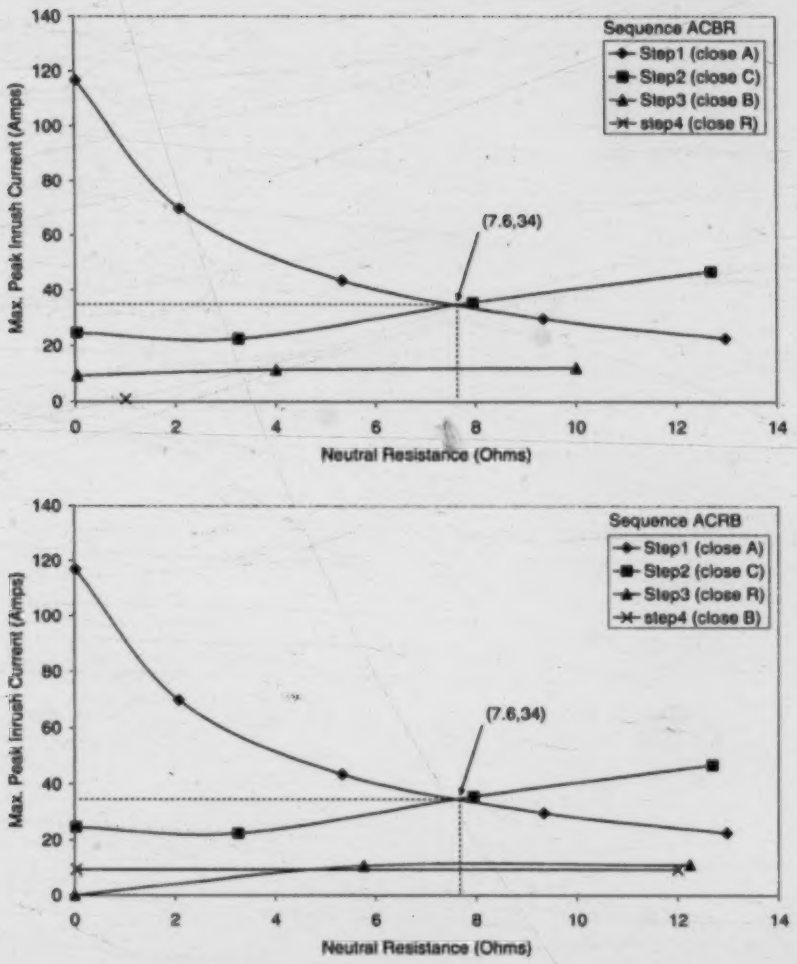

Figure 3.16: Sequence ACBR and ACRB Inrush Current Curves (Neutral Resistor Method)

Figure 3.16 shows that the step three inrush current changes very little as resistance changes. Also, the inrush current in step three is much smaller than the inrush current in steps one and two. The third step is not important in determining an optimal resistance for minimizing the inrush current.

In step four, there were 2 options: close R (ACBR) or close B (ACRB). The effect of closing R will be minimal in a balanced three phase network. This is because the neutral current would be approximately zero and therefore the voltage across the resistor will also be zero. As a result, the step four inrush current does not appear in the ACBR graph. The step four inrush current for the

ACRB sequence appears as a flat line in the graph. This is because the resistor was bypassed in step three, and is no longer part of the circuit. The inrush current is therefore independent of the resistor size.

These results show that sequence ACBR and ACRB are best at minimizing inrush current. Step one and two inrush current curves warrant the most consideration for determining the optimal resistor value to minimize inrush current. By graphing the inrush current curves together versus resistance, the optimal point was found to be approximately 7.6Ω and resulted in 34A peak. Compared to the 94A peak of the direct connection method, this is a 64% reduction. This shows that this method is quite effective in reducing the inrush current of an induction generator when the rotor speed is 1800rpm

3.4 Comparison and Conclusion

From the experiments and discussion in the previous sections, it is clear that the two new proposed methods significantly reduce the peak level of induction generator inrush current. Using the two proposed methods to gradually magnetize the machine through sequential closing of contactors reduces the peak of the inrush current. For each of the experiments, the best sequence was found and the corresponding optimal resistor size was experimentally determined. For all four experiments, the optimal point was determined based on the intersection of the step one and step two inrush current curves. Table 3.5 summarizes the optimal switching sequence and corresponding optimal resistance for each configuration.

Table 3.5: Optimal Sequence and Resistance for Each Configuration at 1800rpm

Series Resistor Method	Optimal Sequence	Optimal Resistance
Delta	CBRA or CARB	5.6Ω
Wye	CBRA or CARB	15.7Ω
Wye grounded	CRBA or CRAB	6Ω
Neutral Resistor Method	ACBR or ACRB	7.6Ω

The effectiveness of these two proposed methods can be measured by comparing them to the direct connection method and the 3 series resistor method. The following figure summarizes the

experimental results and draws a comparison between the proposed methods and the existing methods. The % value in the chart is in relation to the direct connection inrush current.

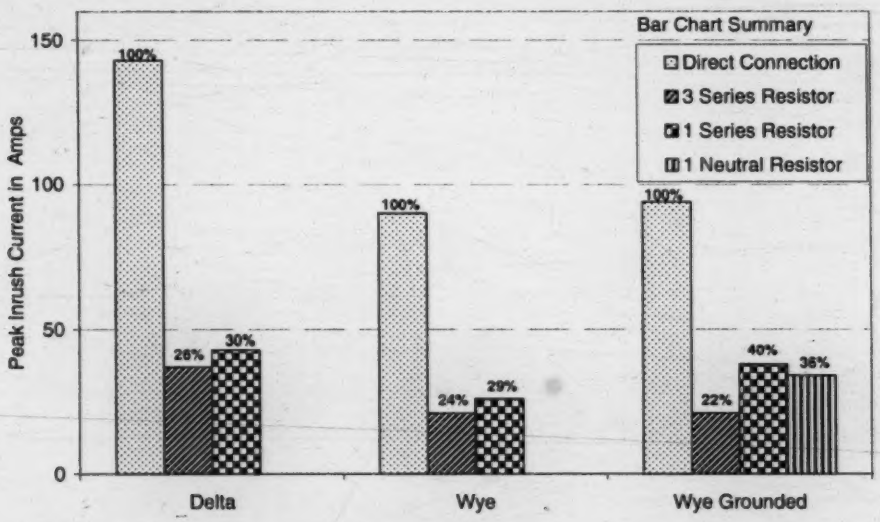

Figure 3.17: Summary of Inrush Current at a Rotor Speed of 1800rpm

The single series resistor method can be used on all three generator configurations (delta, wye, and wye grounded). It was found for the delta configuration, that inrush current can be reduced by 70%. This is only a 4% difference when compared with the 3 series resistor method. Similar results were found for the wye configuration. For the wye grounded configuration, the inrush current was reduced by only 60%. The proposed single series resistor method is therefore most effective if the stator neutral is ungrounded.

The neutral resistor method can only be used on the wye grounded neutral configuration. It was found that this method reduced the inrush current by 64%. It is more effective to use the neutral resistor method rather than the series resistor method when connecting a generator with a wye grounded neutral configuration.

Although the 3 series resistor method reduced inrush current to a slightly greater extent than the proposed methods, the results were comparable. The proposed method offers the advantage of being more cost effective to implement than the 3 series resistor method.

Chapter 4

Simulation Study of the Proposed Methods

In the previous chapter it was experimentally determined that the proposed methods were effective when used on small induction generators. In industry, induction generators much larger than 7.5HP are used to generate electricity. As a result, it is important to see if the proposed methods would be effective when used on large machines. The proposed methods were tested using a much larger induction generator with a power rating of 2MVA. A total of three configurations were evaluated using computer simulations[2]. The simulation results are presented in this chapter. The single series resistor scheme was tested using wye and wye grounded configurations. The third simulation study was conducted on the neutral resistor scheme. This scheme can only be used on a wye grounded generator. The series resistor method using a delta stator was not studied as before because an induction machine model with a delta stator was not available.

4.1 Simulation Setup

The proposed methods call for sequential closing of contactors. As a result, each of the three generator configurations required a series of steps to be completed before being fully connected to the grid. Each step was tested for different resistance values so that the effect of a single

[2] The computer software used for the simulations was PSCAD. PSCAD is well known in industry and is used in power system studies at many universities and utility companies. As a result, PSCAD software has been verified in the past and it was not necessary to verify it again in this work. It should be noted that in this work, there were no major trend differences between the experimental results and simulation results. This fact again verifies the accuracy of PSCAD.

resistor could be determined. When a switch is closed, inrush current occurs in all phases that are energized. The peak inrush current does not necessarily occur in the phase that was switched. Consequently, more than one virtual current probe was required to capture the peak inrush current in each energized phase. When a contactor is closed, it takes some time for the currents and voltages in the generator to reach steady state. Enough time was allowed to elapse between steps to ensure that steady state was reached prior to the closing of contactors in subsequent steps.

The maximum peak inrush current for each step was captured. Unlike the laboratory experiments, it was not necessary to capture 50 waveforms in order to find the maximum peak inrush current. In the experimental method, the moment of switching was random and required a large number of switching events to ensure that the maximum peak inrush current was extracted. In the simulations, the moment of switching can be controlled so the maximum peak inrush current could be successfully obtained with fewer captured waveforms.

The maximum peak inrush current in each step was then plotted versus the resistance. Based on these plots, the resistor value that best minimized the inrush current was extrapolated. The effectiveness of the two new methods was evaluated by comparing the inrush current with the direct connection method and the three series resistor method. The parameters used in the simulation are listed below:

Table 4.1: PSCAD Simulation Parameters

Parameter	**Value**
Rated Power	2MVA
Rated Voltage (Line-Line RMS)	690V
System Frequency	60Hz
System Resistance	0.0001 Ohms
Stator/rotor turns Ratio	0.4333
Stator Resistance	0.0175 pu
Rotor Resistance	0.019 pu
Stator leakage Inductance	0.2571 pu
Rotor leakage Inductance	0.295 pu
Mutual inductance	6.921 pu
Simulation Time Step	35 μs

A fixed rotor speed of 1pu was used. 1pu corresponds to synchronous speed. The system impedance was set to be very low to eliminate voltage drops. The angular moment of inertia and mechanical damping did not affect the simulations, as the rotor speed was fixed. It was justified to use a fixed speed of 1pu because most large machines have a large moment of inertia associated with them. The large mass of the machines rotor will limit rotor speed oscillations. This results in minimal speed variance occurring when connecting the generator to the grid. Thus the speed prior to connection will approximately equal the speed after connection. The tables showing the sequence descriptions are not reiterated in this chapter as they have already been defined in the previous chapter (Table 3.1, Table 3.2, Table 3.3, Table 3.4). All the simulations were conducted using the following line-ground rms voltages: $Ea = 398\angle 0^{\circ}$, $Eb = 398\angle -120^{\circ}$, $Ec = 398\angle +120^{\circ}$.

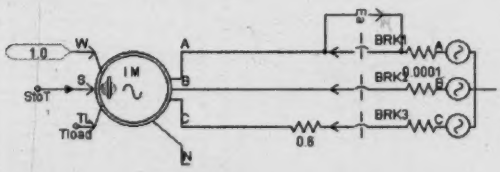

(a) Series resistor method with Wye Config.

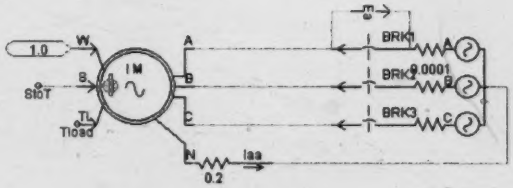

(b) Neutral resistor method

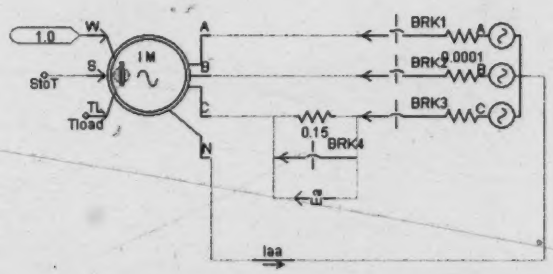

(c) Series resistor method with Wye Grounded Config.

Figure 4.1: Screen Shots of Simulation Setup in PSCAD

The direct connection method and the three series resistor method were also simulated to allow comparisons to be drawn with the two proposed methods. The same results will be obtained for all three configurations when using either the direct connection method or the three series resistor method because the voltage source and the induction machine are balanced. As a result, no

current will flow in the neutral phase. From the simulation results, the maximum peak inrush current using the direct connection method was found to be 7923A. The three series resistor method reduced the maximum peak inrush current to 1530A when a $0.333\,\Omega$ resistor was placed in each phase. These results were obtained without the installation of PF correction capacitors.

4.2 Single Series Resistor Method

The single series resistor method was tested on two stator configurations: wye and wye grounded neutral.

4.2.1 Wye Configuration

The simulation results are shown in Figure 4.2. Recall that for the wye configuration, sequence CBRA and CARB will yield the same results.

Figure 4.2 shows that the sequences that best minimize the peak inrush current are sequence CBRA and CARB. Both of these sequences consist of bypassing the resistor in the second step. Using either of these two sequences minimizes the inrush current to 1800A at a series resistor value of $0.457\,\Omega$. This is a reduction of 77% when compared to the direct connection method. The optimal point occurs when the step one and step two inrush current curves intersect. The step one inrush current decreases as the series resistance increases. However, (except for a small portion of the graph in CABR) as the resistance increases, so does the inrush current in the step two. This is why the optimal point for all three sequences is the intersection of the step one and step two inrush current. The step three inrush current is relatively low and does not affect the selection of the optimal resistor value.

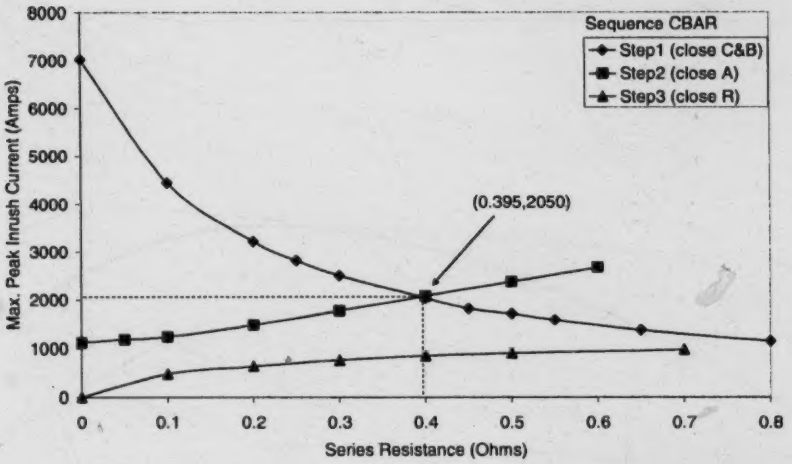

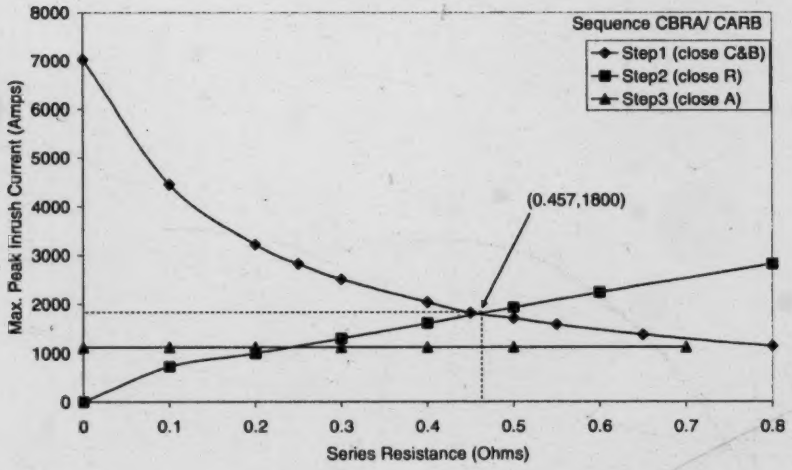

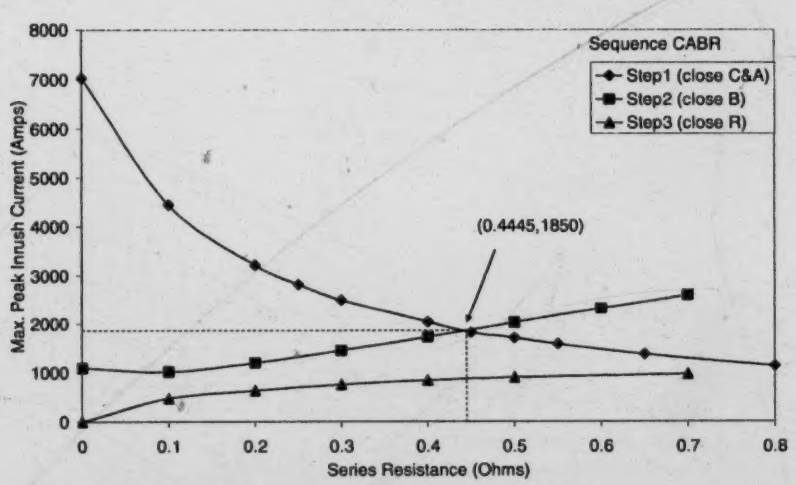

Figure 4.2: Simulated Inrush Current Curves (Wye Configuration)

4.2.2 Wye Grounded Configuration

Similar to the wye simulation, only the first two steps were required to determine the optimal point. The first two steps are plotted in the following figure.

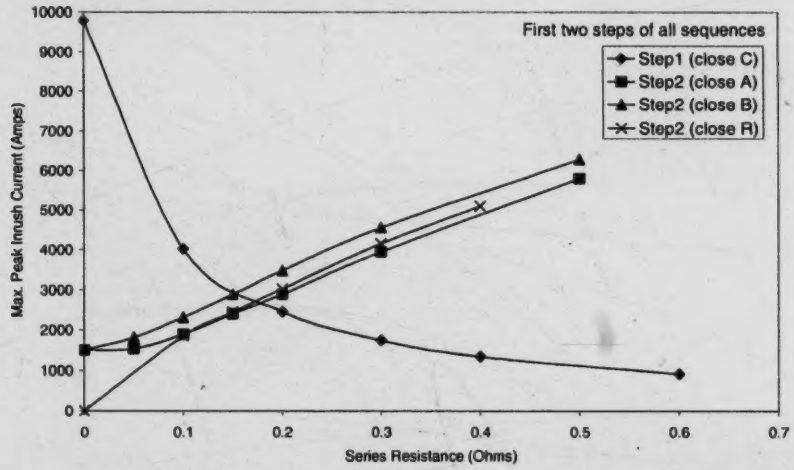

Figure 4.3: Step One and Two Inrush Current Curves (Wye Grounded Configuration)

From Figure 4.3, there are three optimal points. The optimal point that yields the smallest current is the intersection of step one inrush current and the step two inrush current when phase A is closed in step two. As a result the sequence that best minimizes the inrush current is either sequence CABR or sequence CARB. It can be seen from Figure 4.4 that both of these sequences produce relatively small inrush current in steps three and four. The step four inrush current for sequence CARB is a straight line because the resistor was bypassed in step three and is no longer part of the circuit. As a result, the step four inrush current does not depend on the series resistance value. The optimal point of these two sequences occurred when a series resistor value of $0.1785\,\Omega$ was used. This resistance value minimized the maximum peak inrush current to approximately 2678A. This is a reduction of 66% when compared to the direct connection method.

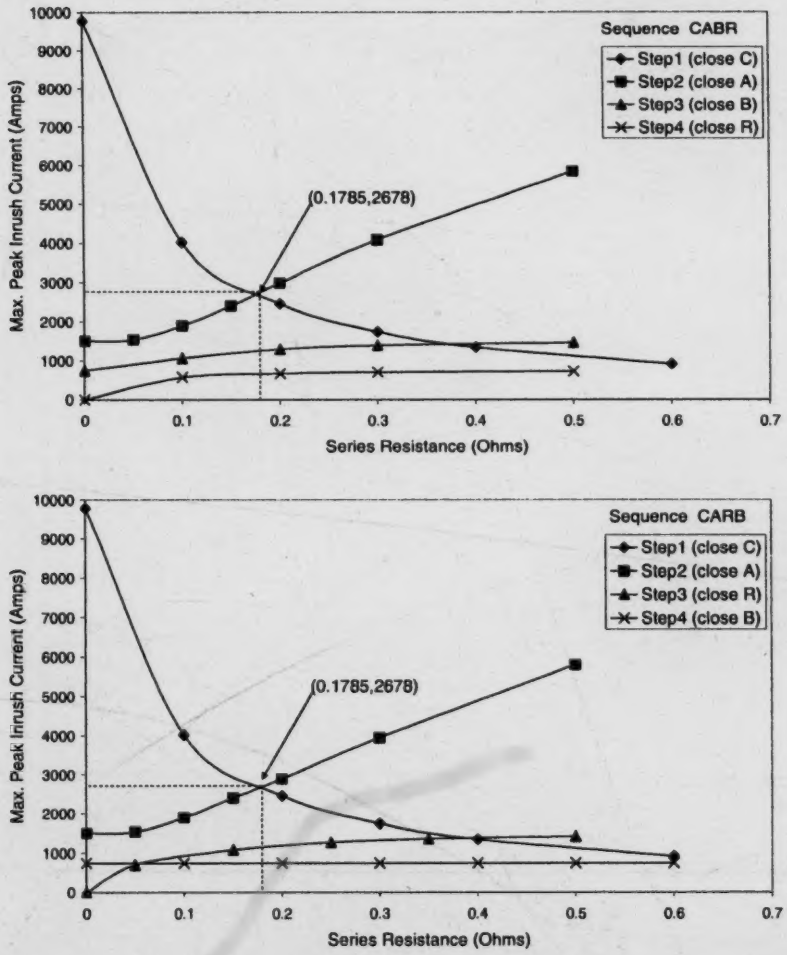

Figure 4.4: Sequence CABR and CARB Inrush Current Curves (Wye Grounded Config.)

4.3 Neutral Resistor Method

This simulation was completed on a wye neutral grounded induction generator model. The neutral resistor was placed between the neutral terminal of the generator and the grounded point of the system. Similar to single series resistor simulation, only the first two steps were required to determine the optimal point. The inrush current curves for the first two steps are plotted in the following figure.

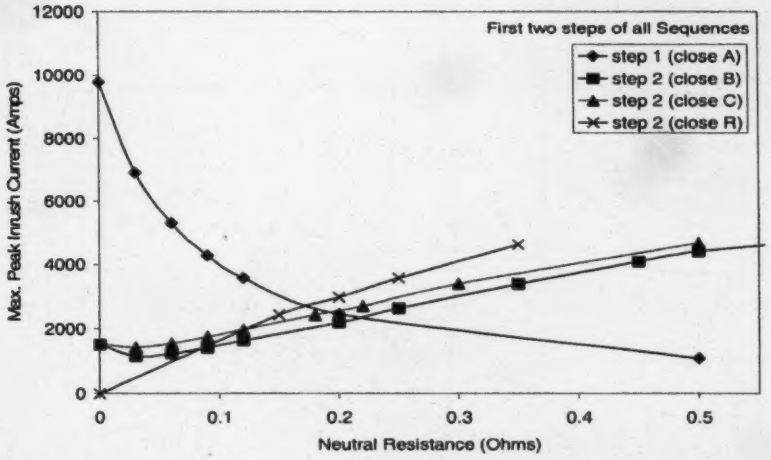

Figure 4.5: Step One and Two Inrush Current Curves (Neutral Resistor Method)

From Figure 4.5, there are three optimal points. The optimal point that yields the smallest current is the intersection of the step one inrush current and the step two inrush current when phase B is closed in step two. As a result, the sequence that best minimizes the inrush current is either sequence ABCR or sequence ABRC. For both sequences, the third and fourth steps produce relatively small inrush current (see Figure 4.6). The step four inrush current for sequence ABCR is not shown in Figure 4.6 because there is no inrush current when bypassing a neutral resistor of a fully balanced machine. The step four inrush current for sequence ABRC is a straight line because the resistor was bypassed in step three and is no longer part of the circuit. As a result, the step four inrush current is independent of the neutral resistance value. The optimal point of these two sequences occurred when a series resistor value of 0.218Ω was used. This resistance value minimized the peak inrush current to 2350A. This is a reduction of 70% when compared to the direct connection method.

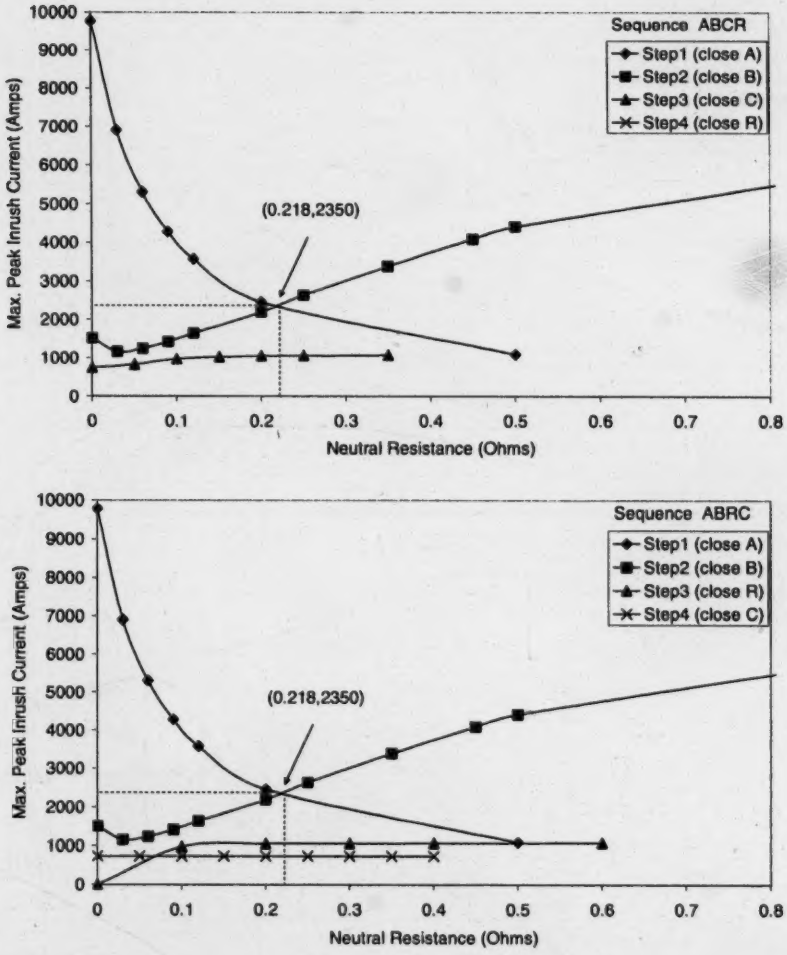

Figure 4.6: Sequence ABCR and ABRC Inrush Current Curves (Neutral Resistor Method)

4.4 Comparison and Conclusion

In this chapter the proposed methods were simulated to determine if they were effective. In order to measure the effectiveness of the two methods, the inrush current results need to be compared to the direct connection method and the three series resistor method. The direct connection method and the three series resistor method were tested using an ungrounded wye induction generator. The rotor speed was fixed at 1pu. It was found that using the direct connection method produced a maximum peak inrush current of about 7923A. The three series resistor method could reduce

the maximum peak inrush current to 1530A when a resistance of 0.333 Ω was placed in each phase. The results are summarized in Figure 4.7.

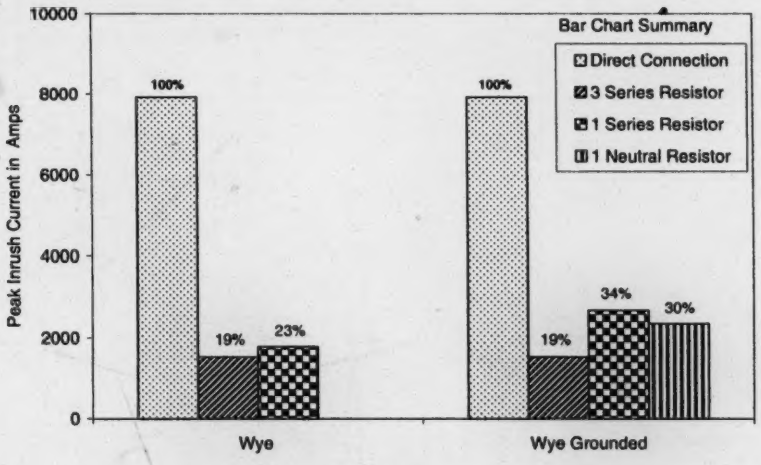

Figure 4.7: Summary of Inrush Current at a Rotor Speed of 1800rpm

Using the single series resistor method reduced the inrush current in the wye ungrounded machine to 23%. This is comparable to results of using the three series resistor method. On the wye grounded configuration, the neutral resistor method reduced the inrush current to 30%. These results are slightly more favorable than the single series resistor method, which reduced the inrush current to 34%. The traditional three series resistor method performed the best when compared to the two proposed methods. From the simulation results, it has been shown that the proposed methods are almost as effective as the three series resistor method in reducing induction generator inrush current.

From the intersection point of the step one and two inrush current curves, the required resistance value that best minimizes the inrush current curve was extrapolated. This optimal point depends on the contactor closing sequence. The sequence that yielded the smallest inrush current was determined as shown in Table 4.2.

For the wye configuration with a single series resistor, the sequences that best minimized inrush current were CBRA and CARB. For the wye grounded configuration with a single series resistor, the best sequences were CABR and CARB. For the neutral resistor method, the best sequences were ABCR and ABRC.

Table 4.2: Optimal Sequence and Resistance for Each Configuration at 1800rpm

Series Resistor Method	Optimal Sequence	Optimal Resistance
Wye	CBRA or CARB	0.457Ω
Wye grounded	CABR or CARB	0.1785Ω
Neutral Resistor Method	ABCR or ABRC	0.218Ω

So far, only the simulation results of connecting an induction generator to the grid at a constant rotor speed of 1pu have been presented. Computer simulations were also conducted at the following rotor speeds: 0.97, 0.985, 1.015 and 1.03pu. For the simulations, the rotor speed was held constant throughout the experiments. In reality, however, the rotor speed might not remain constant for speeds less than 1pu. For example, closing the contactors in step one may cause the machine to accelerate. Only the sequences that were optimal at 1pu were tested at these rotor speeds. Figure 4.8 shows how the optimal resistor changes with rotor speed. Figure 4.9 shows the maximum peak inrush current that occurs when the optimal resistor is inserted in the circuit.

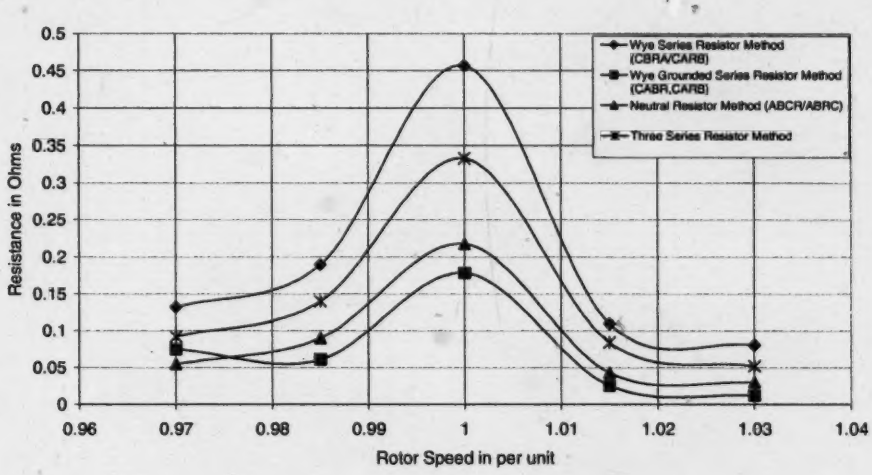

Figure 4.8: Optimal Resistance versus Rotor Speed

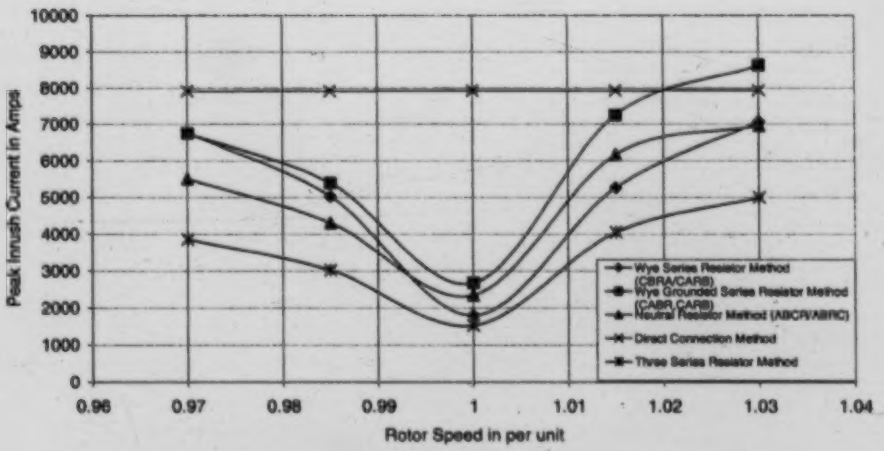

Figure 4.9: Maximum Peak Inrush Current versus Rotor Speed

From Figure 4.9, the maximum peak inrush current for the direct connection method remains almost constant for different rotor speeds. For all other methods, the inrush current increases as the rotor speed moves further away from 1pu. As a result, for all methods except for the direct connection method, the maximum peak inrush current is best minimized when the rotor speed is approximately 1pu.

Chapter 5

Steady State Analysis

In the previous two chapters it was shown (experimentally and using computer simulations) that the two proposed methods were effective at reducing the maximum peak inrush current in induction generators for all 4 stator configurations. The inrush current was reduced when compared to the direct connection method. Each stator configuration had an optimal sequence, as well as an optimal resistance value. The first goal of this chapter is to take one of the stator configurations and show why certain sequences were better than others. The stator configuration that was chosen was the wye grounded configuration with a single series resistor. The first goal is achieved using the steady state principle of superposition. As shown in this chapter, it was found that the steady state voltages can determine what sequence is best. This leads to the second goal of this chapter, which is to derive equations that describe the steady state operation of an unbalanced induction generator. This allows steady state voltages to be obtained theoretically so that the optimal sequence can be determined using only these equations. It is also shown in this chapter that the steady state equations can be used to determine the rotor speed that can minimize the inrush current.

5.1 Transient Analysis Using Superposition

It was previously found that the most severe inrush current occurs in steps one and two. The first step requires closing the phase in which the series resistor is placed. In this case, C was arbitrarily chosen for the location of the resistor. The second step can be either to close A, B or R. It was found from the computer simulations that closing contactor A in step two caused the least amount of inrush current. This section explains why closing phase A results in a smaller inrush current than closing phase B in step two. The electrical circuit after step one is shown in Figure 5.1.

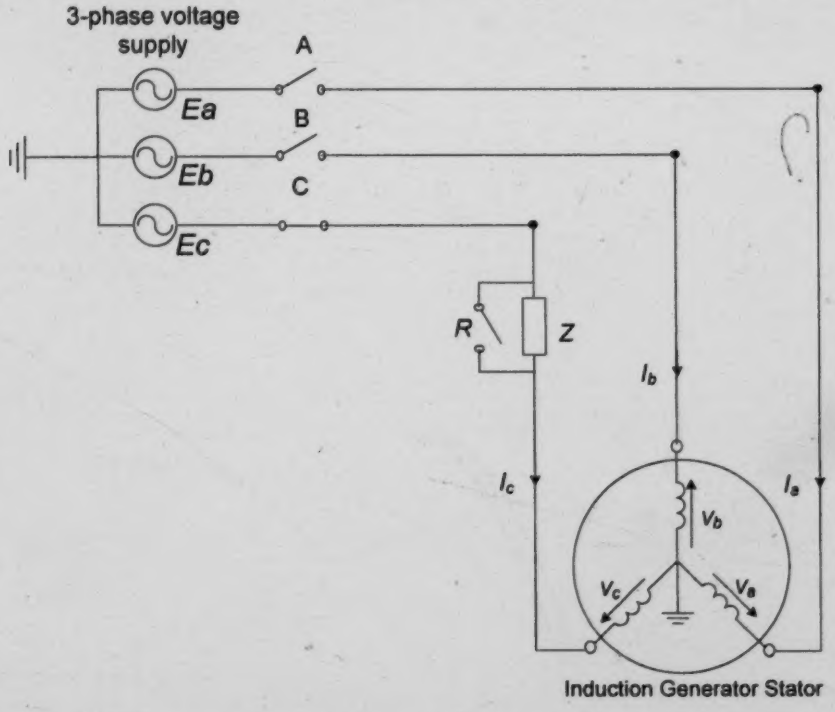

Figure 5.1: Wye Grounded Configuration with Series Resistor After Step One

The circuit can be simplified as shown in Figure 5.2.

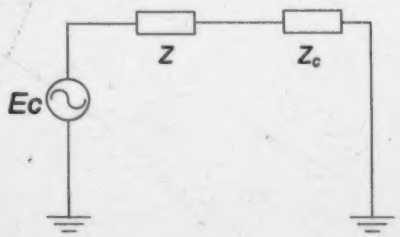

Figure 5.2: Simplified Circuit with only Phase C Closed

In the previous figure, Z is the external series impedance, which in our case, is a resistor. Z_c is the phase C impedance of the induction machine. The phase C stator winding has a steady state current as a result of the system line to ground voltage. The stator current, in turn, induces current in the rotor. The rotor current induces a voltage (V_a and V_b) across the phase A and B stator windings. However, since A and B are not closed yet, no current flows in the phase A and B windings. Since steady state voltages are induced in the phase A and B stator windings, the open contactor voltage is much less than the line to ground voltage of the system. The voltages across the contactors in phase A and phase B are given as:

$$\begin{aligned} \Delta V_A &= Ea - V_a \\ \Delta V_B &= Eb - V_b \end{aligned} \tag{5.1}$$

where Ea and Eb are the system line to ground voltages and V_a and V_b are the induced stator voltages in phase A and B respectively as shown in Figure 5.1. The closer the stator and system voltages are to one another in both magnitude and phase, the smaller the voltage across the contactor will be.

We can analyze the circuit at the instant the second switch is closed by using the principle of superposition. This principle states that the total response of a linear system with more than one voltage source can be obtained by summing the responses of each individual voltage source in the circuit. Figure 5.3(a) shows the circuit at the moment phase A is closed in step two. ΔV_A is the rms voltage across contactor A prior to switching. Z_a and Z_c are the stator winding impedances found in phase A and C respectively.

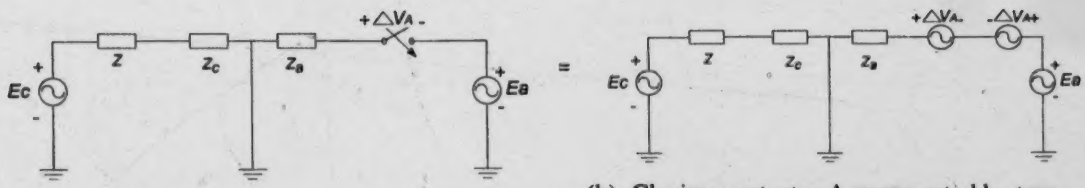

(a) Closing contactor A

(b) Closing contactor A represented by two opposing voltage sources

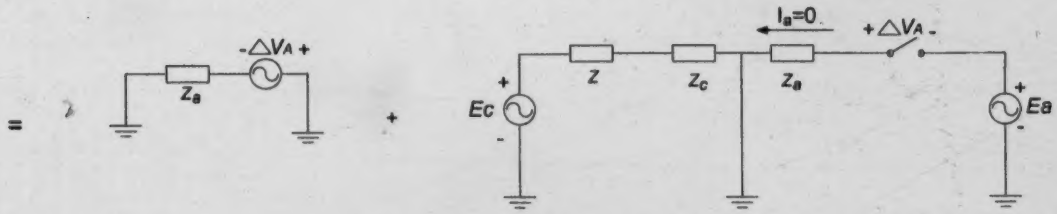

(c) Application of superposition

Figure 5.3: Application of Superposition when Closing Contactor A in Step Two

Once the switch is closed, the voltage drop across the contactor becomes zero and can be represented by two opposing voltage sources as shown in Figure 5.3(b). Figure 5.3(c) shows that the circuit at the instant of switching can be represented by the summation of two circuits. The first circuit is composed of the stator impedance in series with a voltage source with value, ΔV_A. The second circuit is the same circuit that exists prior to closing A. The current, I_a, in this second circuit is zero. Therefore, the inrush current in phase A is equal to the current of the first circuit. The first circuit is composed of a voltage source in series with the phase A stator winding impedance, which is composed of a resistance and an inductance:

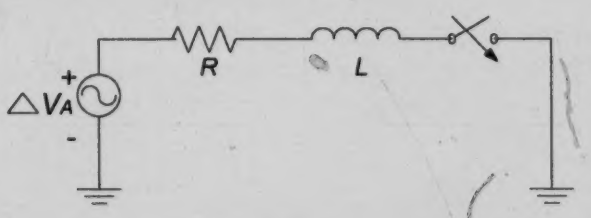

Figure 5.4: Equivalent Circuit when Closing Contactor A in Step Two

The largest possible inrush current of the previous circuit is given in [23] as:

$$i_a(t) = \sqrt{2}\frac{\Delta V_A}{\sqrt{R^2 + L^2}}\left[\sin(wt - \frac{\pi}{2}) + e^{\frac{t}{L/R}}\right] \tag{5.2}$$

where $i(t)$ is the current flowing in the circuit once the switch is closed at time t=0 and ΔV_A is the steady state rms voltage across contactor A prior to switching.

Similarly, if contactor B is closed in step two, the equation describing the largest possible inrush current can be given as:

$$i_b(t) = \sqrt{2}\frac{\Delta V_B}{\sqrt{R^2 + L^2}}\left[\sin(wt - \frac{\pi}{2}) + e^{\frac{t}{L/R}}\right] \tag{5.3}$$

These equations are valid assuming that R and L do not change. It can be assumed that the circuit for the first cycle does not change significantly after the switching event, and that R and L are constant. It can also be assumed that R and L in equations 5.2 and 5.3 are the same since the machine is symmetrical.

From computer simulations, the steady state voltages across contactors A and B were found at different resistor values. The voltages are plotted in the Figure 5.5 along with the maximum peak inrush current plots previously shown in Chapter 4.

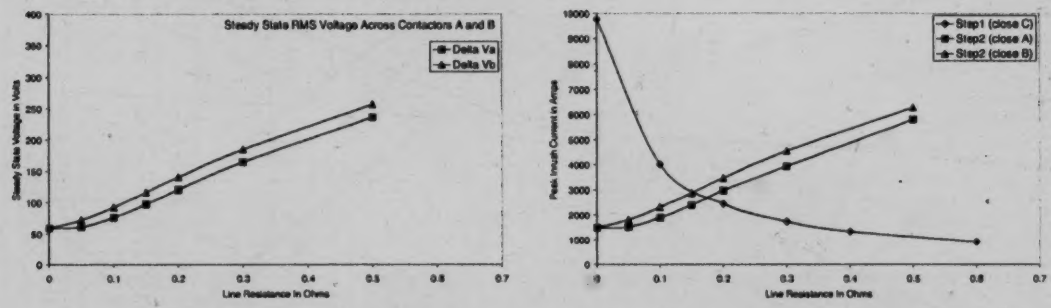
Steady State RMS Voltage Across Contactors A and B
Delta Va
Delta Vb
Steady State Voltage in Volts
Line Resistance in Ohms
Step1 (close C)
Step2 (close A)
Step2 (close B)
Peak Inrush Current in Amps
Line Resistance in Ohms

Figure 5.5: Steady State Voltages and Inrush Current Associated with Step Two

From the previous figure, the peak inrush current in phase A and B are very similar in shape to the steady state voltage across contactors A and B prior to switching. After step one, the steady state voltage across contactor B is larger than the steady state voltage across A. This translates to a larger peak inrush current in phase B than in phase A. To clearly see the relationship between the voltages and the peak inrush current, equations 5.2 and 5.3 are combined into the following equation:

$$\frac{\Delta V_B}{\Delta V_A} = \frac{i_b(t)}{i_a(t)} \tag{5.4}$$

Closing contactor A in step two means that the current in phase A reaches its peak after some time $t_{PEAK\ A}$. Closing contactor B in step two means that the current in phase B reaches its peak after some time $t_{PEAK\ B}$. According to equations 5.2 and 5.3, the time it takes for the current to reach its peak value when A is closed, is the same as when B is closed. That is, $t_{PEAK\ A} = t_{PEAK\ B}$. Therefore, equation 5.4 can be re-written as:

$$\frac{\Delta V_B}{\Delta V_A} = \frac{i_b(t_{PEAK\ B})}{i_a(t_{PEAK\ A})} = \frac{i_{b\ Maximum\ Peak\ inrush}}{i_{a\ Maximum\ Peak\ inrush}} \tag{5.5}$$

The ratio of ΔV_A to ΔV_B and $i_{a\ Maximum\ Peak\ inrush}$ and $I_{b\ Maximum\ Peak\ inrush}$ found from the computer simulations are given in the following table.

Table 5.1: Relationship Between Steady State Voltage and Inrush Current

Series Resistance	V_b/V_a	I_b/I_a
0	1.0047506	1.004765711
0.05	1.1727689	1.177499386
0.1	1.212963	1.219023749
0.15	1.1956522	1.201007939
0.2	1.1637427	1.164995116
0.3	1.1218884	1.121665
0.5	1.0868263	1.076133447

Table 5.1 shows that the ratio of the steady state voltages is approximately equal to the ratio of the maximum peak inrush current. Therefore the equations obtained in this section are accurate.

Another important observation from Figure 5.5 is that the open contactor voltages both for contactor A and B tend to increase as the external series resistor impedance increases. Although a large resistance can minimize the step one inrush current, it may also maximize the step two inrush current. This explains why the optimum point occurs when the step one and step two inrush current curves intersect.

The single series resistor method with a grounded neutral configuration requires sequential closing of contactors. The inrush currents that occur in step one and two are the most severe. When the first contactor is closed, steady state voltages are induced in all the stator windings. The voltage across the contactor is dependant on the voltage induced in the winding which is dependant on the external resistance value. It was found that the smaller the rms voltage across the contactor prior to switching, the smaller the peak inrush current. The computer simulations show that the voltage across contactor A was smaller than the voltage across contactor B for all resistance values except zero, in which case, the voltages were identical. This is why closing contactor A in step two yielded a smaller inrush current than closing contactor B in step two.

5.2 Unbalanced Induction Machines

In the previous section it was shown that knowing the steady state voltages across a contactor is useful for determining the optimal sequence for minimizing inrush current in an induction generator. It is therefore beneficial to derive equations that describe the operation of an unbalanced induction machine in steady state.

Using just one resistor and closing contactors sequentially results in an unbalanced induction machine and causes asymmetrical stator voltages. In the past, the method of symmetrical components has been used to derive equations that describe induction machine operation with unbalanced voltages. This method relies on the following theories: a) an asymmetrical system consisting of three phase vector quantities may be replaced by three symmetrical systems of positive, negative and zero sequence and b) that the effect of the asymmetrical system is the summation of the separate effects of the three symmetrical systems [24].

The positive, negative and zero sequence circuits of an induction machine have been derived in [25] and are shown in Figure 5.6.

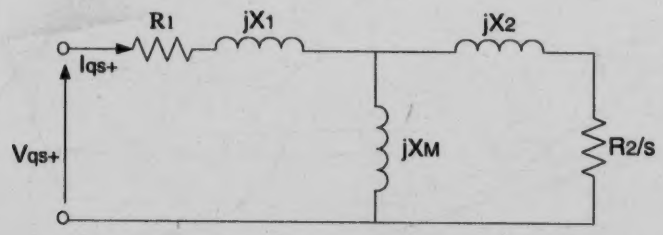

(a) Positive-sequence

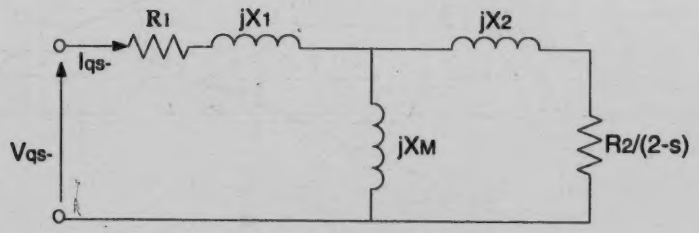

(b) Negative-sequence

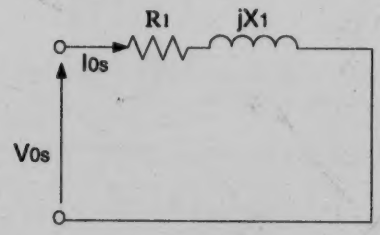

(c) Zero-sequence

Figure 5.6: Induction Machine Symmetrical Component Equivalent Circuits

The positive, negative and zero sequence voltages and currents are related to the actual stator phase voltages and currents by the following equations:

$$\begin{bmatrix} F^s_{qs+} & F^s_{qs-} & F^s_{0s} \end{bmatrix}^T = \frac{1}{3}\begin{bmatrix} 1 & a & a^2 \\ 1 & a^2 & a \\ 1 & 1 & 1 \end{bmatrix} \cdot \begin{bmatrix} F_{as} & F_{bs} & F_{cs} \end{bmatrix}^T \qquad (5.6)$$

and inversely,

$$\begin{bmatrix} F_{as} & F_{bs} & F_{cs} \end{bmatrix}^T = \begin{bmatrix} 1 & 1 & 1 \\ a^2 & a & 1 \\ a & a^2 & 1 \end{bmatrix} \cdot \begin{bmatrix} F^s_{qs+} & F^s_{qs-} & F^s_{0s} \end{bmatrix}^T \qquad (5.7)$$

where $a = e^{j\frac{2\pi}{3}}$ and F can be either voltage or current.

The circuits shown in Figure 5.6 have been used in many papers and text books for steady state analysis including [24], [26] and [27]. These circuits can be used to calculate the steady-state operation of an induction machine with unbalanced stator voltages. The only condition for the circuits to be valid is that the rotor circuit must be symmetrical.

In this chapter, equations describing the unbalanced stator voltages and current are derived for the wye grounded stator configuration when using the proposed series resistor method. This is done using the method of symmetrical components.

5.3 Wye Grounded Neutral Steady State Analysis

The proposed methods introduce asymmetrical primary connections due to having a single resistor and sequential closing of contactors. This results in unbalanced stator voltages and currents. The single series resistor method with a grounded neutral configuration is shown in Figure 5.7. This method requires a total of 4 switching events in order to be normally connected to the grid. Until all four switches are closed, unbalanced voltages and currents exist.

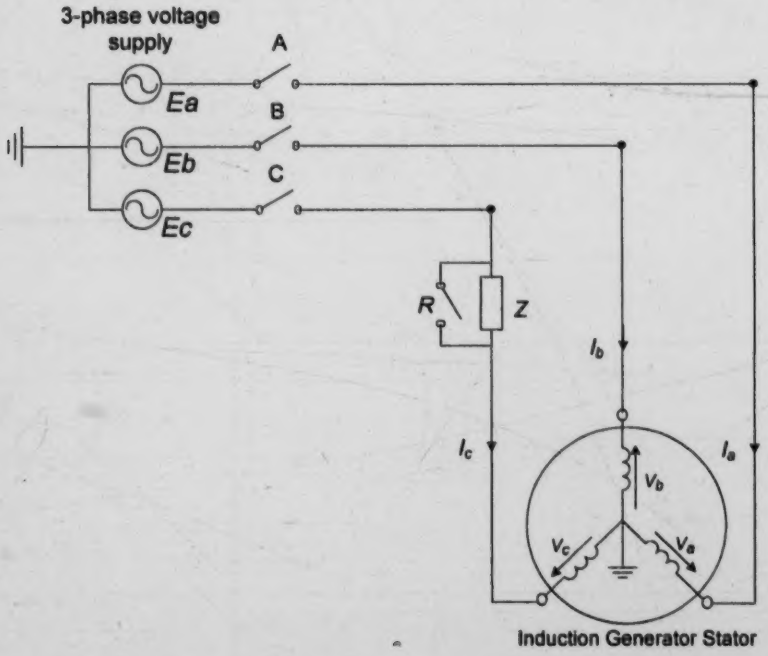

Figure 5.7: Single Series Resistor Method with Grounded Neutral Configuration

Table 5.2: Possible Sequences

Sequence	STEP 1	STEP2	STEP 3	STEP4
CBAR	C	B	A	R
CBRA	C	B	R	A
CABR	C	A	B	R
CARB	C	A	R	B
CRBA	C	R	B	A
CRAB	C	R	A	B

From the equivalent circuits shown in Figure 5.6, the symmetrical component voltages can be written as a product of the symmetrical component circuit impedance and the current.

$$\begin{aligned} V_{qs+} &= I_{qs+} \cdot Z_{qs+} \\ V_{qs-} &= I_{qs-} \cdot Z_{qs-} \\ V_{qs0} &= I_{qs0} \cdot Z_{qs0} \end{aligned} \tag{5.8}$$

Substituting (5.8) into (5.7):

$$\begin{bmatrix} V_a & V_b & V_c \end{bmatrix}^T = \begin{bmatrix} 1 & 1 & 1 \\ a^2 & a & 1 \\ a & a^2 & 1 \end{bmatrix} \cdot \begin{bmatrix} I_{qs+} \cdot Z_{qs+} & I_{qs-} \cdot Z_{qs-} & I_{qs0} \cdot Z_{qs0} \end{bmatrix}^T \tag{5.9}$$

and directly from (5.7):

$$\begin{bmatrix} I_a & I_b & I_c \end{bmatrix}^T = \begin{bmatrix} 1 & 1 & 1 \\ a^2 & a & 1 \\ a & a^2 & 1 \end{bmatrix} \cdot \begin{bmatrix} I_{qs+} & I_{qs-} & I_{qs0} \end{bmatrix}^T \tag{5.10}$$

Substituting (5.9) and (5.10) into the steady-state constraint equations will allow us to solve for the positive, negative and zero sequence currents. The actual stator currents and terminal voltages can then be found via equations (5.9) and (5.10).

In Figure 5.7, there are four switches that need to be closed in order to fully connect the induction generator to the grid. This is done in 4 steps, with a total of 6 possible sequences as shown in Table 5.2. Prior to each step, constraint/inspection equations can be obtained from Kirchoffs voltage laws. These equations change depending on which contactors are closed. As a result, the steady state voltage and currents will be obtained for each possible connection of the induction generator. The steady state equations and results after step one are shown in this chapter. For the steady state equations and results after step two and step three please refer to the Appendix.

5.3.1 Steady State Equations After Step One

Step one consists of closing the contactor that will connect the source voltage with the resistor. This was contactor C. The constraint equations are:

$$\begin{aligned} Ec &= I_c Z + V_c \\ I_a &= I_b = 0 \end{aligned} \tag{5.11}$$

Since $I_a = I_b = 0$, then $I_{qs+} = a^2 \frac{I_c}{3}$, $I_{qs-} = a\frac{I_c}{3}$, $I_{qs0} = \frac{I_c}{3}$ from equation (5.6).

From equation (5.9), $V_c = \frac{I_c}{3}\left(Z_{qs+} + Z_{qs-} + Z_{qs0}\right)$.

Simplified, we have the following equation:

$$I_c = \frac{Ec}{Z + \frac{Z_{qs+} + Z_{qs-} + Z_{qs0}}{3}} \tag{5.12}$$

The stator voltages and currents can be found using equations (5.9) and (5.10). Once the stator voltages are known, the open contactor voltage across contactor B (ΔV_B), A (ΔV_A) and the voltage across the series resistor (ΔV_R) can be found using the following equations:

$$\begin{aligned} \Delta V_R &= (I_c)Z \\ \Delta V_A &= Ea - V_a \\ \Delta V_B &= Eb - V_b \end{aligned} \tag{5.13}$$

Expanding equations (5.13) yields the following equations:

$$\Delta V_R = \left(\frac{Ec}{Z + \frac{Z_{qs+} + Z_{qs-} + Z_{qs0}}{3}} \right) Z$$

$$\Delta V_A = Ea - \left(\frac{Ec}{Z + \frac{Z_{qs+} + Z_{qs-} + Z_{qs0}}{3}} \right) \left(\frac{a^2 Z_{qs+} + aZ_{qs-} + Z_{qs0}}{3} \right) \quad (5.14)$$

$$\Delta V_B = Eb - \left(\frac{Ec}{Z + \frac{Z_{qs+} + Z_{qs-} + Z_{qs0}}{3}} \right) \left(\frac{aZ_{qs+} + a^2 Z_{qs-} + Z_{qs0}}{3} \right)$$

5.4 Validation of Steady State Equations

In the previous section, the steady state equations that describe the wye grounded configuration with a series resistor have been given. To verify that these equations are correct, the steady state voltages and currents after step one of the computer simulation are compared with the steady state values calculated from the equations derived in this section. Comparison of the steady state voltages and currents after step two and three are shown in the Appendix.

As long as the motor parameters are known, the steady state analysis of the machine can be calculated using the derived equations. For the simulated induction machine, the positive and negative sequence parameters are exactly the same (see Table 5.3).

Table 5.3: Simulated Induction Machine Parameters

Parameters in Ohms	Positive Sequence	Negative Sequence	Zero Sequence
R_1 = stator resistance	0.004165875	0.004165875	0.004165875
R_2 = referred rotor resistance	0.004523	0.004523	-
X_1 = stator leakage reactance	j 0.0612	j0.0612	j0.0612
X_2 = referred rotor leakage reactance	j 0.07022475	j 0.07022475	-
X_M = magnetizing reactance	j 1.6475	j1.6475	-

The source voltage used in the equations were of the same magnitude as the source voltages used in the computer simulation: $Ea = 398\angle 0^{\circ}$, $Eb = 398\angle -120^{\circ}$ and $Ec = 398\angle +120^{\circ}$. The steady state voltage and current rms values of the induction machine were found using the derived equations. The results are compared with the steady state values obtained from the computer simulations in Figure 5.8, Figure A1 and Figure A2. When plotting the voltages at speeds of 1pu, an approximate speed of 0.999pu was used. This is because at 1pu, slip is zero and the positive sequence circuit becomes undefined. The values in the following figure were obtained using a rotor speed of 1pu.

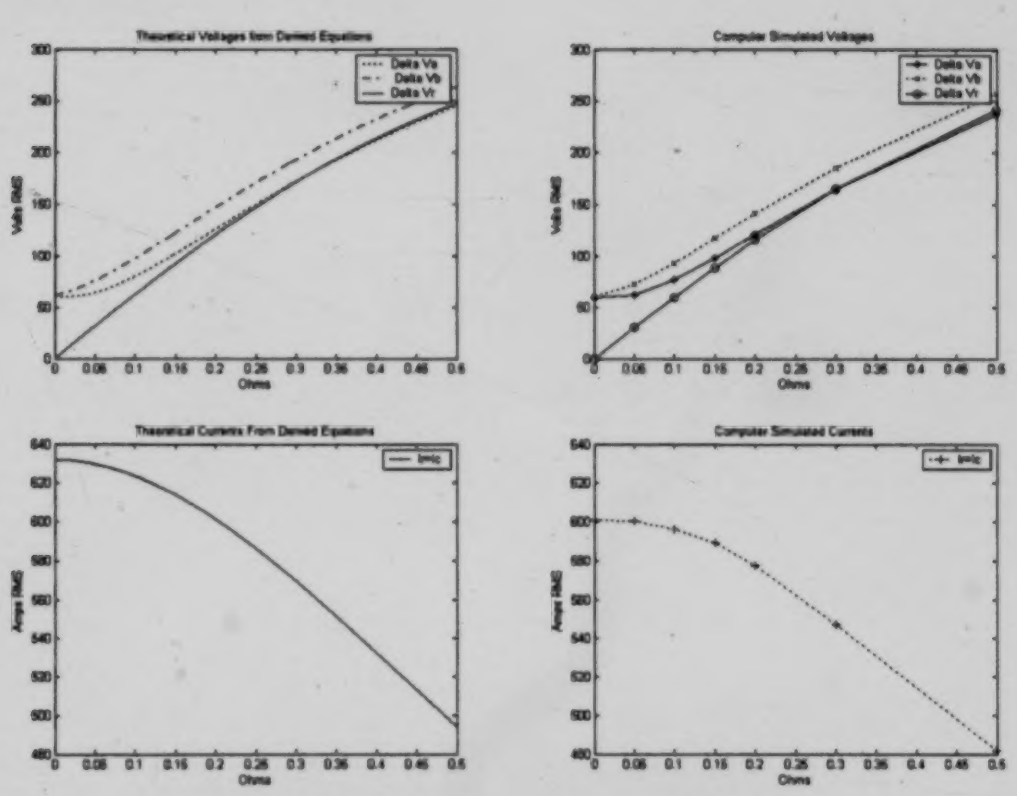

Figure 5.8: Steady State Voltage and Current after Step One

Figure 5.8 shows the steady state rms currents and open contactor voltages after step one. The currents and voltages are dependant on the resistor value. The figures also show that the equations are very accurate since the results very closely resemble the results found using the computer simulation. The slight differences may be attributed to the simulation time step, interpolation and round off error. Another observation is that the open contactor voltages are much smaller after

step two and three than after step one (see Appendix). This could be one of the reasons why the inrush currents in step three and four are much smaller than the step one and two inrush currents.

In the computer simulations, the positive and negative sequence parameters, R_1, R_2, X_1, X_2 and X_M were set to be the same. However this is not the case in real induction machines, where the positive and negative sequences parameters are different from each other. When an induction machine is supplied by asymmetrical stator voltages, the rotor currents are made up of two frequencies. These are:

$\omega - \omega_r$ due to the positive and zero sequence components and
$\omega + \omega_r$ due to the negative sequence component

As a result, the positive sequence voltage will yield low rotor frequencies, and the negative sequence voltage component will yield high rotor frequencies. It is well known that the rotor circuit resistance and inductance varies as the frequency changes. In order to have accurate results using the equations, it is necessary to know the positive and negative sequence impedances. This can be done by conducting a locked rotor test at 15Hz to find the approximate positive sequence parameters, and at 120Hz to find the approximate negative sequence rotor parameters. As an example, the positive and negative parameters for the experimental machine are given in Table 5.4.

Table 5.4: Experimental Induction Machine Parameters

Parameters all in Ohms	Positive Sequence	Negative Sequence	Zero Sequence
R_1 = stator resistance	0.825	0.825	0.825
R_2 = referred rotor resistance	0.6	3.271	-
X_1 = stator leakage reactance	j2	j2	j2
X_2 = referred rotor leakage reactance	j3	j1.11	-
X_M = magnetizing reactance	j54	j54	-

5.5 Steady State Voltage and Inrush Current as Rotor Speed Changes

The results in chapter 3 and 4 showed that the optimal resistance values are specific to individual rotor speeds. If, however, the rotor speed is not the same as the selected speed, large inrush current can occur, rendering the proposed method ineffective. This section will provide some analysis of the series resistor method with a wye grounded configuration at different fixed rotor speeds.

The steady state equations derived in this chapter (equations 5.14) show that the steady state voltages and currents are a function of the source voltage, motor parameters, external series resistance value, and the rotor speed. The source voltage is fixed, as are the motor parameters. As a result, the steady state voltage and current is only dependant on the rotor speed and the external resistance value. It was already concluded in this chapter that the maximum peak inrush current in step two, is dependant on the open contactor voltage, which is dependant on rotor speed. It can therefore be concluded that the rotor speed plays a large role in determining the inrush current in step two.

After step one, there is current flowing in the energized phase of the induction generator, which induces current in the rotor. The magnitude and phase angle of this current is dependant upon the rotor speed. This rotor current, in turn, induces voltage across the un-energized stator windings. The closer the terminal voltage is to the source voltage, the smaller the voltage across the contactor will be. The smaller the steady state voltage across a contactor prior to closing, the smaller the subsequent peak inrush current will be. This was shown in the previous sections using the principle of superposition. Since the rotor speed affects the stator voltage, it also affects the open contactor voltage. At a rotor speed of 1pu, the wye grounded configuration with a series resistor best reduced inrush current when contactor A was closed in step two. At 1pu, the optimal resistor size was approximately $0.1785\,\Omega$. The equation describing the steady state voltage across contactor A prior to step two is given again in equation 5.15.

$$\Delta V_A = Ea - \left(\frac{Ec}{Z + \frac{Z_{qs+} + Z_{qs-} + Z_{qs0}}{3}} \right) \left(\frac{a^2 Z_{qs+} + aZ_{qs-} + Z_{qs0}}{3} \right) \qquad (5.15)$$

The positive and negative sequence impedance is dependant on the rotor speed and so, the voltage across contactor A prior to step two is also dependant on the rotor speed. The steady state voltage across contactor A is shown in Figure 5.9.

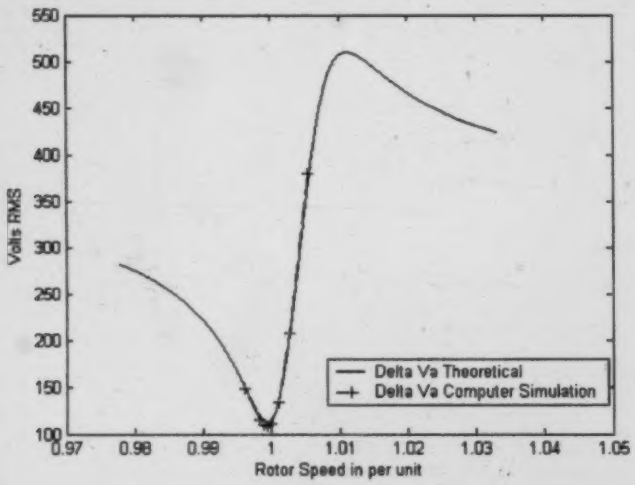

Figure 5.9: Delta V_a as a Function of Rotor Speed, Series Resistor R=0.1785 Ω

Both the computer simulated voltages and the theoretical voltages are shown in the figure. Figure 5.9 shows that the voltage across the contactor is minimal at slightly less than synchronous speed (1pu). As expected, the peak inrush current when closing contactor A in step two is minimized when the steady state voltage prior to closing the switch is minimized. This is shown in following figure.

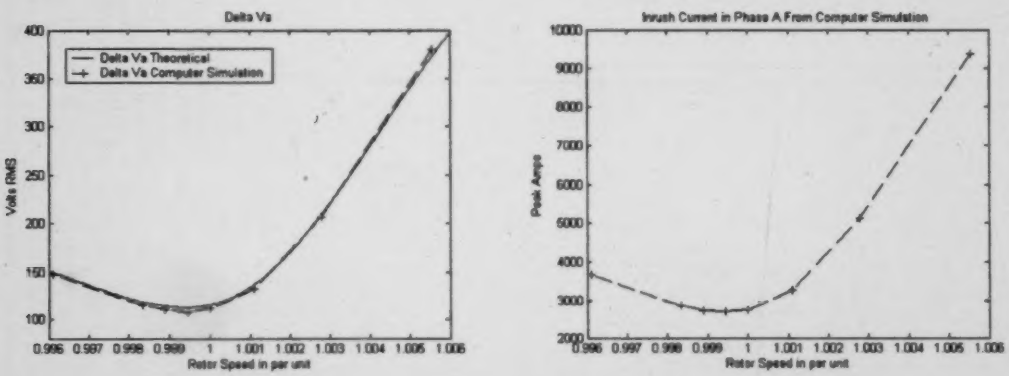

Figure 5.10: Steady State Voltage prior to Closing A and Max. Peak Inrush after Closing A

The graphs also show that as the rotor speed strays from the minimal point in either direction, inrush current increases. This rise in inrush current value is much more prominent when contactor A is closed at speeds greater than the minimal point. It is therefore necessary to ensure that the rotor speed is monitored and controlled properly during the connection procedure. Fortunately, induction generator installations have a governor that can control rotor speed by changing the mechanical settings of the prime mover.

5.6 Summary

In this chapter, steady state analysis was carried out on an induction generator with a wye grounded configuration and a series resistor. The purpose of the steady state analysis was to find the relationship between open contactor voltages and inrush current. When connecting the generator using this configuration, closing contactor B in step two would cause a larger inrush current than closing contactor A. Steady state analysis showed that the larger inrush current from closing B was due to the larger steady state voltage across the contactor prior to closing. The optimal sequence may therefore be determined based on the steady state voltage prior to closing. It should be noted that $\Delta V_A \leq \Delta V_B$ when the rotor speed was 1pu and results will vary with different rotor speeds and different induction generator parameters.

It was beneficial to derive equations that describe an unbalanced induction machine to allow steady state voltages and currents to be determined without experimentation or computer simulation. These equations were derived using the method of symmetrical components. The steady state voltages and currents were then plotted versus the external series resistor value and compared to the steady state voltages and currents obtained from computer simulations. The results were very similar, thereby verifying the equations. The relationship between the rotor speed and inrush current was also shown.

Chapter 6

Conclusions and Future Work

Voltage sags that occur due to induction generator connection to the grid can be severe and can lead to poor power quality levels in a power system. Methods of limiting induction generator inrush current already exist and have been discussed in this work. However, these methods are often expensive and complicated. This work proposes two new methods that are more cost effective and more simple than previous methods.

The primary goal of this work was to present and validate the effectiveness of two new methods. This goal was achieved through extensive testing both experimentally in a laboratory, and theoretically using computer simulations. Induction generators can have different stator windings, and as a result, the proposed methods were tested on three different stator configurations. The test results show that the 2 proposed methods provide an effective and less costly means of connecting induction generators to the grid than the traditional methods.

Once the proposed methods were validated, a steady state analysis was done on the wye grounded configuration with a series resistor. It was found that the inrush current after closing a contactor was dependant on the steady state voltage across the contactor prior to its closing. Larger voltages caused larger inrush currents, while smaller voltages caused smaller inrush currents. Following this observation, equations were derived to serve as a more efficient way of determining the steady state voltages and currents after each step. This was done using the method of symmetrical

components. The equations were then verified by comparing them to computer simulation results. Although not shown in this work, other configurations can also be analyzed in steady state using symmetrical components.

The only known disadvantage of the two proposed methods is the unbalanced voltages that are induced in the stator by the sequential closing of the contactors. These unbalances can cause negative and/or zero sequence current to flow in the machine. This in turn causes heating [28,29] and mechanical torque oscillations. Large shaft torque transients are harmful to the gear box [18]. Future research can be conducted to measure problematic over-heating and torque oscillations.

In this work, all experiments were done without the connection of power factor correction capacitors. It has been shown in [18] that PF correction capacitors can help further reduce inrush current when used in conjunction with the three series resistor method. Future research may be conducted to test if PF correction capacitors can help further reduce inrush current when using the methods proposed in this thesis. If so, there would be no significant increase in cost since induction generator installations commonly have capacitor banks installed to improve other power quality issues. As a result, it may be possible to further reduce the inrush current without increasing cost.

Bibliography

[1] L. Chang, H. M. Kojabadi, "Review of interconnection standards for distributed power generation," *in Proceedings of the IEEE 2002 Large Engineering Systems Conference on Power Engineering*, 2002.

[2] W. Freitas, E. Asada, A. Morelato, W. Xu, "Dynamic improvement of induction generators connected to distribution systems using a DSTATCOM," *IEEE International Conference on Power System Technology*, vol. 1, pp. 173-177, 13-17 Oct. 2002.

[3] L. Wang, Y. Yang, S. Kuo, "Analysis of Grid-connected Induction Generators Under Three-Phase Balanced Conditions," *IEEE Power Engineering Society Winter Meeting*, vol. 1, pp. 413-417, 27-31 Jan. 2002.

[4] P. Sen., J. Nelson, "Application guidelines for induction generators" *IEEE International Conference on Electric Machines and Drives*, 18-21 May 1997.

[5] S. S. Murthy, C. S. Jha, P. S. Nagendra, "Analysis of grid connected induction generators driven by hydro/wind turbines under realistic system constraints," *IEEE Transaction on Energy Conversion*, vol. 5, no. 1. March 1990.

[6] M. F. McGranaghan, D. R. Mueller, M. J. Samotyj, "Voltage sags in industrial systems," *IEEE Transactions on Industry Applications.*, vol. 29, no. 2, March/April 1993.

[7] V.E. Wagner, A. A. Andreshak, J.P. Staniak, "Power Quality and Factory Automation," *IEEE Transactions on Industry Applications*, vol. 26, no. 4, pp. 620–626, July-Aug. 1990.

[8] D. O'Kelly, *Performance and Control of Electrical Machines,* London: McGraw-Hill, pp 256- 257, 1991.

[9] Y. Sasaki, N. Harada, T. Kai, T. Sato, "A Countermeasure against the voltage sag due to an inrush current of wind power generation system interconnecting to a distribution line," *T.IEE Japan*, vol. 120-B, no. 2, pp. 180-186, 2000.

[10] K. Sasaki, T. Matuzaka, K. Tsuchiya, "Voltage fluctuation simulation of power system due to a wind driven induction generator," *T.IEE Japan*, vol, 110-B, no. 1, pp. 33-39, 1990.

[11] T. Senjyu, N. Sueyoshi, K. Uezato, H. Fujita, "Transient current analysis of induction generator for wind power generating system," *IEEE Asia Pacific Conference and Exhibition on Transmission and Distribution*, vol. 3, pp.1647-1652, Oct. 2002.

[12] R.C. Dugan, M.F. McGranaghan, H.W. Beaty, *Electrical Power Systems Quality*, New York: McGraw-Hill, 1996.

[13] L. Guasch, F. Corcoles, J. Pedra, "Effects of unsymmetrical voltage sag types E, F and G on induction motors," *in Proceedings of the Ninth International IEEE Conference on Harmonics and Quality of Power*, vol. 3, pp.796-803, Oct. 2000.

[14] S. J. Chapman, *Electric Machine Fundamentals*, Third Edition, McGraw-Hill 1999.

[15] K. D. Pham, "Cogeneration application: Interconnection of induction generators with public electric utility," *IEEE 35th Annual Rural Electric Power Conference*, pp. D4/1-D4/7, 28-30 April 1991.

[16] T. J. Hammons, S.C. Lai, "Voltage dips due to direct connection of induction generators in low head hydro electric scheme," *IEEE Transactions on Energy Conversion*, vol. 9, no. 3, September 1994.

[17] V. Pongpornsup, B. Eua-Arporn, "Impacts of non-utility induction generator to distribution network," *IEEE/PES Transmission and Distribution Conference and Exhibition 2002: Asia Pacific*. vol. 2, pp. 1352-1356, 6-10 Oct. 2002.

[18] T. Thiringer, "Grid-Friendly connecting of constant speed wind turbines using external resistors," *IEEE Transactions on Energy Conversion*, vol. 17, no. 4, December 2002.

[19] A. G. Gonzalez Rodriguez, M. Burgos Payan, C. Izquierdo Mitchell, "PSCAD based simulation of the connection of a wind generator to the network", *IEEE Porto Power Tech Conference*, Portugal, 10-13 September 2001.

[20] S. A. Gomez, J. L. R. Amenedo, "Grid Synchronisation of doubly fed induction generators using direct torque control," *IEEE 28th Annual Conference of the Industrial Electronics Society*, vol. 4, pp. 3338-3343, 5-8 Nov. 2002.

[21] C. Sankaran, (2002), *Power Quality*, CRC Press [Online]. Available: http://www.engnetbase.com.

[22] K.J.P. Macken, M.H.J. Bollen, R.J.M. Belmans, "Mitigation of voltage dips through distributed generation systems," *IEEE 38th IAS Annual Meeting*, vol. 2, pp. 1068-1074. 12-16 Oct. 2003.

[23] J. D. Glover, M. S. Sarma, *Power System Analysis and Design*,3rd edition, Brooks/Cole 2002.

[24] J. E. Brown, O. I. Butler, "A general method of analysis of three-phase induction motors with asymmetrical primary conditions," *IEE Proceedings*, vol. 100, Part II, pp. 25-34, February 1953.

[25] P. C. Krause, "The method of symmetrical components derived by reference frame theory," *IEEE Transaction on Power Apparatus and Systems*, vol. PAS–104, no. 6, June 1985.

[26] A. Tozune, "Balanced operation of three-phase induction motor with asymmetrical stator windings connected to a single-phase supply system," *IEE Proceedings-B*, vol. 138, no.4, July 1991.

[27] P. C. Krause, *Analysis of Electric Machinery*, McGraw-Hill, 1986.

[28] J. Marczewski, "Utility Interconnection Issues," *IEEE Power Engineering Society Summer Meeting*, vol. 1, pp. 439 – 444, 18-22 July 1999.

[29] R. Barnes, K. Wong, "Unbalance and harmonic studies for the channel tunnel railway system," *IEE Proceedings-B*, vol. 138, no. 2, pp. 41-50, March 1991.

Appendix

Wye grounded induction machine with single series resistor: Derivation of Steady State Equations after Step two and three

Steady State Equations After Step Two

Step two consists of closing either A , B, or bypassing the resistor. Bypassing the resistor will yield the same equations as (5.12) with Z=0. The constraint equations after closing A are:

$$\begin{aligned} Ec &= I_c Z + V_c \\ Ea &= V_a \\ I_b &= 0 \end{aligned} \qquad \text{(A.1)}$$

Substituting (5.9) and (5.10) into (A.1) yields the following equation:

$$\begin{bmatrix} Ec \\ Ea \end{bmatrix} = \begin{bmatrix} Z + \frac{Z_{qs+}}{3} + \frac{Z_{qs-}}{3} + \frac{Z_{qs0}}{3} & \frac{aZ_{qs+}}{3} + \frac{a^2 Z_{qs-}}{3} + \frac{Z_{qs0}}{3} \\ \frac{a^2 Z_{qs+} + aZ_{qs-} + Z_{qs0}}{3} & \frac{Z_{qs+} + Z_{qs-} + Z_{qs0}}{3} \end{bmatrix} \begin{bmatrix} I_c \\ I_a \end{bmatrix} \qquad \text{(A.2)}$$

Since all source voltages and sequence impedances are known, I_c and I_a can be found by taking the inverse of the matrix. Once the currents are known, the stator voltages can be found using equation (5.9) and (5.10). Once the stator voltages are known, the open contactor voltage across contactor B (ΔV_B), and the voltage across the series resistor (ΔV_R) can be found using the following equations:

$$\begin{aligned} \Delta V_R &= (I_a)Z \\ \Delta V_B &= Eb - V_b \end{aligned} \qquad \text{(A.3)}$$

If in step 2, contactor B is closed instead of contactor A, the constraint equations will be:

$$\begin{aligned} Ec &= I_c Z + V_c \\ Eb &= V_b \\ I_a &= 0 \end{aligned} \tag{A.4}$$

Substituting (5.9) and (5.10) into (A.4) yields the following equation:

$$\begin{bmatrix} Ec \\ Eb \end{bmatrix} = \begin{bmatrix} Z + \frac{Z_{qs+}}{3} + \frac{Z_{qs-}}{3} + \frac{Z_{qs0}}{3} & \frac{a^2 Z_{qs+}}{3} + \frac{aZ_{qs-}}{3} + \frac{Z_{qs0}}{3} \\ \frac{aZ_{qs+} + a^2 Z_{qs-} + Z_{qs0}}{3} & \frac{Z_{qs+} + Z_{qs-} + Z_{qs0}}{3} \end{bmatrix} \begin{bmatrix} I_c \\ I_b \end{bmatrix} \tag{A.5}$$

Since all source voltages and sequence impedances are known, I_c and I_b can be found by taking the inverse of the matrix. Once the stator currents are known, the stator voltages can be found using equation (5.9) and (5.10). Once the stator voltages are known, the open contactor voltage across contactor A (ΔV_A), and the voltage across the series resistor (ΔV_R) can be found using the following equations:

$$\begin{aligned} \Delta V_R &= (I_a)Z \\ \Delta V_A &= Ea - V_a \end{aligned} \tag{A.6}$$

Steady State Equations After Step Three and Four

Step three consists of either closing A, B or bypassing the resistor. Bypassing the resistor will yield the same solutions as after step two, with Z=0. Closing A or B means that all the contactors are closed except for R. The constraint equations are:

$$\begin{aligned} Ec &= I_c Z + V_c \\ Eb &= V_b \\ Ea &= V_a \end{aligned} \tag{A.7}$$

Substituting (5.9) and (5.10) into (A.7) yields the following equation:

$$\begin{bmatrix} Ec \\ Eb \\ Ea \end{bmatrix} = \begin{bmatrix} aZ + aZ_{qs+} & a^2 Z + a^2 Z_{qs-} & Z + Z_{qs0} \\ a^2 Z_{qs+} & aZ_{qs-} & Z_{qs0} \\ Z_{qs+} & Z_{qs-} & Z_{qs0} \end{bmatrix} \begin{bmatrix} I_{qs+} \\ I_{qs-} \\ I_{qs0} \end{bmatrix} \tag{A.8}$$

The sequence currents can be found by taking the inverse of the above matrix. Then the stator voltages and currents can be obtained using equations (5.9) and (5.10).

After step four, the induction machine will be connected normally to the grid without any series impedance.

The following figures are the steady state voltages and currents after step two and three. The steady state values obtained from the derived equations are very similar to the steady state values obtained from the computer simulations. Therefore, the equations derived are accurate.

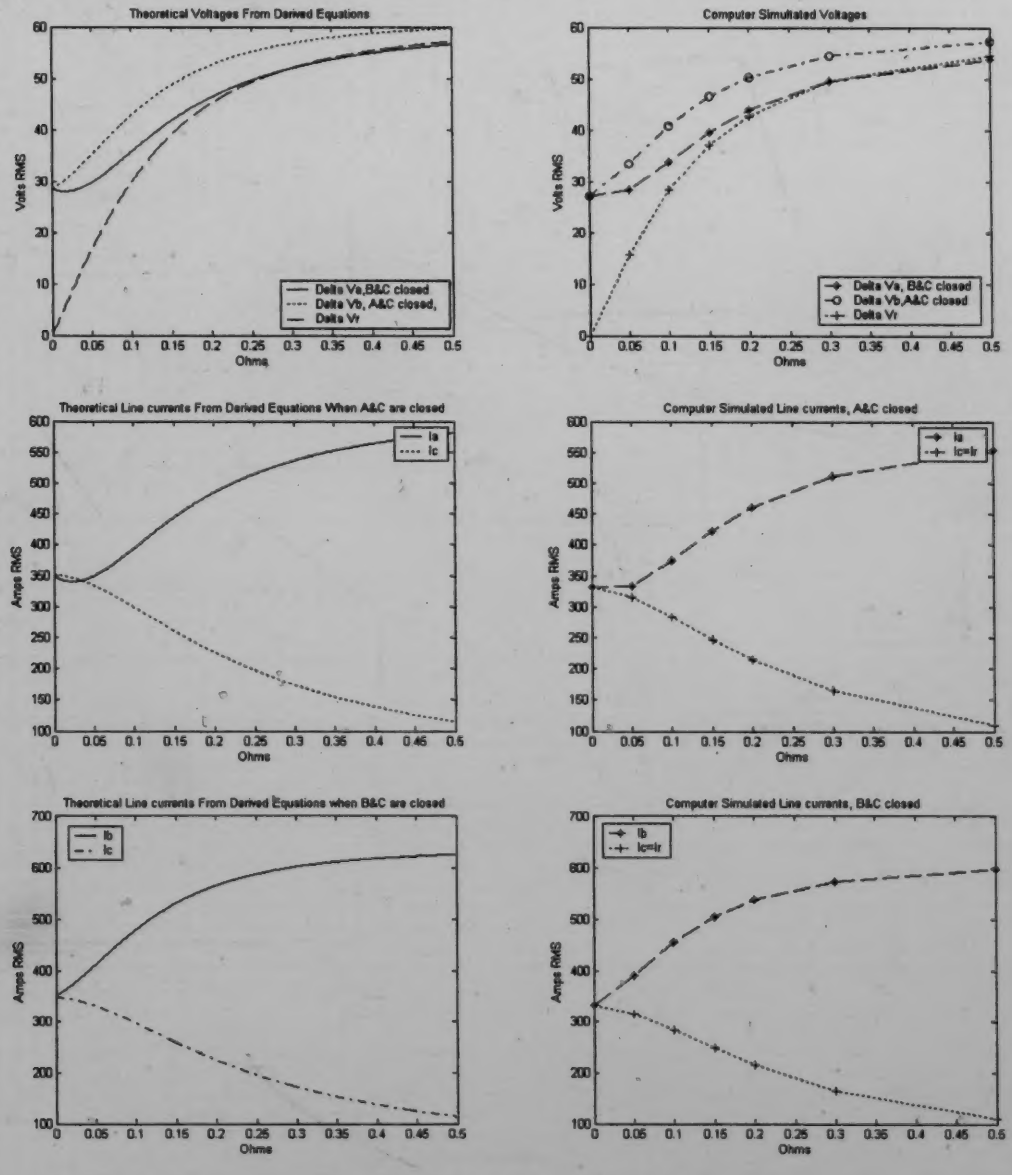

Figure A1: Steady State Voltage and Current After Step Two

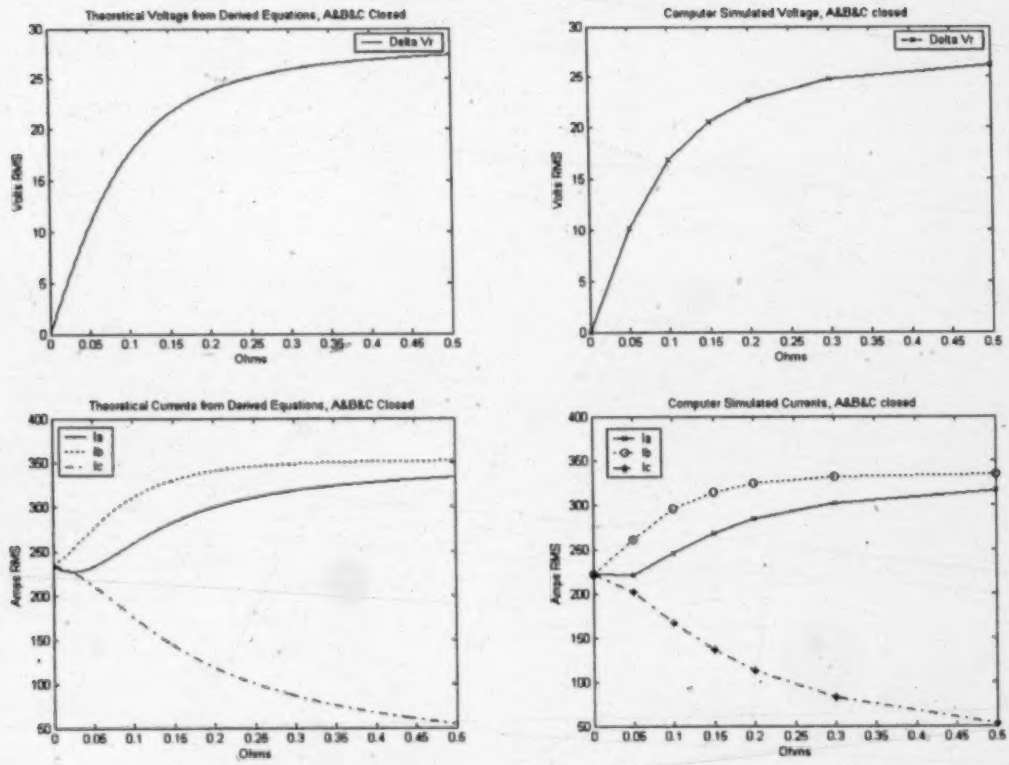

Figure A2: Steady State Voltage and Current After Step Three